Article

A new frog family (Anura: Terrarana) from South America and an expanded direct-developing clade revealed by molecular phylogeny

MATTHEW P. HEINICKE[1], WILLIAM E. DUELLMAN[2], LINDA TRUEB[2], D. BRUCE MEANS[3], ROSS D. MacCULLOCH[4], & S. BLAIR HEDGES[1,5]

[1]*Department of Biology, 208 Mueller Laboratory, The Pennsylvania State University, University Park, PA 16802, USA.*
E-mail: mph177@psu.edu, sbh1@psu.edu

[2]*University of Kansas Natural History Museum and Biodiversity Research Center, 1345 Jayhawk Blvd., Lawrence KS 66045, USA.*
E-mail: duellman@ku.edu, trueb@ku.edu

[3]*Coastal Plains Institute, 1313 Milton Street, Tallahassee, FL 32303, USA. E-mail: means@bio.fsu.edu*

[4]*Department of Natural History, Royal Ontario Museum, 100 Queen's Park, Toronto, ON M5S 2C6, Canada.*
E-mail: rossm@rom.on.ca

[5]*Corresponding author. E-mail:sbh1@psu.edu.*

Table of contents

Abstract

Three frogs of a new species found in cloud forests on two nearby mountains in Guyana were included in a molecular phylogeny of 17 nuclear and mitochondrial genes (10,739 aligned sites) that revealed that their closest relative is Terrarana (Brachycephalidae, Craugastoridae, Eleutherodactylidae, and Strabomantidae) and their next-closest relative is Hemiphractidae (marsupial frogs). We place these frogs in a new family, genus, and species which is strongly supported as the basal clade within Terrarana: Ceuthomantidae n. fam., *Ceuthomantis smaragdinus* **n. gen**, **n. sp.** Morphological evidence supports the placement of two other species from the Guiana Highlands, *Pristimantis aracamuni* (Barrio-Amorós & Molina) and *P. cavernibardus* (Myers & Donnelly), in the new family and genus. This close phylogenetic relationship of terraranans and marsupial frogs, nearly all of which have direct development, supports an hypothesis that direct development evolved early in the evolution of this huge clade (~1000 species), for which we propose the unranked taxonomic epithet Orthobatrachia.

Key words: Amphibia, Ceuthomantidae, Guyana, Hemiphractidae, Nobleobatrachia, Orthobatrachia, Terrarana

Resúmen

Tres ranas encontradas en los bosques de niebla de dos montañas cercanas de la Guayana fueron incluidas en una filogenia molecular de 17 genes nucleares y mitocondriales (10,739 caracteres alineados). La filogenia revel que los parientes más cercanos de estas ranas son los Terrarana (Brachycephalidae, Craugastoridae, Eleutherodactylidae, y Strabomantidae), y los siguientes más cercanos son los hemifractidos. Describimos estas ranas como una nueva especie, y creamos un nuevo género y una familia para acomodarla: Ceuthomantidae **fam. nov.**, Ceuthomantis smaragdinus **gen. nov.**, **sp. nov.** La posición basal de la nueva familia dentro de Terrarana est bien apoyada. La evidencia morfológica apoya la inclusión de otras dos especies de las tierras altas guayanesas, Pristimantis aracamuni (Barrio-Amorós & Molina) y P. cavernibardus (Myers & Donnelly) en la nueva familia y en el nuevo género. La hemandad filogenética entre Terrarana y las ranas marsupiales, prácticamente todas con desarrollo directo, apoya la hipótesis de la aparición temprana del desarrollo directo en la evolución de este enorme clado (~ 1000 especies), para el cual proponemos el epíteto sin rango de Orthobatrachia.

Palabras clave: Amphibia, Ceuthomantidae, Guayana, Hemiphractidae, Nobleobatrachia, Orthobatrachia, Terrarana

Introduction

During the past five years, phylogenetic studies of frogs based on molecular data have resulted in many taxonomic changes at the familial and generic levels—Darst and Cannatella 2004, Faivovich *et al.* 2005, Wiens *et al.* 2005, Frost *et al.* 2006, Grant *et al.* 2006, Crawford & Smith 2005, and Guayasamin *et al.* 2008. Frogs formerly placed in the immense, diverse genus *Eleutherodactylus* were subjected to phylogenetic analyses of both mitochondrial and nuclear genes by Hedges *et al.* (2008). The analysis of 344 species resulted in the recognition of four families (Brachycephalidae, Craugastoridae, Eleutherodactylidae, and Strabomantidae) placed in the unranked taxon Terrarana, with one "unknown Anuran sp." (Hedges *et al.*, 2008, fig. 2) lying between Terrarana and the outgroups. This unidentified juvenile frog resembled *Pristimantis,* by far the largest genus in the Strabomantidae with 426 species (AmphibiaWeb 2009); this small frog was found on Mt. Ayanganna, Guyana, by A. Lathrop and C. Cox in October 2000. In July 2007 one of us (D.B.M) collected several species of *Pristimantis* on nearby Mt. Kopinang, Guyana. Genetic sequences obtained from tissues of these specimens revealed that two individuals were essentially the same as the "unknown anuran." Morphologically, the frogs resembled some species of *Pristimantis*. However, the phylogenetic analyses of sequences from 17 genes revealed that these specimens are not only distinct from Strabomantidae but represent an evolutionary lineage so distant that its closest relative is the clade containing all terraranan frogs (i.e., 4 families and ~900 species). Unique morphological traits further supported their position in the molecular tree and showed that they necessitate placement in a new family, which is described herein.

Materials and methods

General. In the field, specimens were handled and euthanized according to approved animal care protocols. After tissues were removed and placed in 95% ethanol, specimens were fixed in formalin and subsequently stored in 70% ethanol. We use the classification proposed by Hedges *et al.* (2008). Museum abbreviations are: AMNH = American Museum of Natural History, New York, USA; KU = Herpetological collection in the Biodiversity Institute (formerly Natural History Museum), University of Kansas, Lawrence, USA; MVZ = Museum of Vertebrate Zoology, University of California, Berkeley, USA; ROM = Royal Ontario Museum, Toronto, Canada.

Morphology. External observations and measurements were taken under a Leica stereo-zoom microscope. Measurements were taken to the nearest 0.1 mm with dial calipers. Measurements and external

morphological features are those defined by Lynch and Duellman (1997), except that the term dentigerous processes of vomers is used instead of vomerine odontophores. Snout–vent length is abbreviated SVL. In order to maintain consistency, the numbered arrangement in the diagnosis also follows that in Lynch and Duellman (1997). Sex was determined by examination of the gonads. The nature of the adductor musculature and of the glandlike protrusions on the dorsum was determined by dissection of KU 315000.

We follow Myers and Donnelly's (1997) terminology for emarginate conditions of digital tips: An indented margin is defined as a broad, shallow concavity—e.g., *Pristimantis crenunguis* (Lynch) (Lynch & Duellman 1997, fig. 15C). A notched margin is defined as a distinct, narrow concavity—e.g., *Pristimantis aracamuni* (Barrio-Amorós & Molina 2006, fig. 2); *P. cavernibardus* (Myers & Donnelly 1997, fig. 37A). In *Dischidodactylus duidensis* (Rivero), the ungual flap is indented and longitudinally divided (Lynch 1979, fig. 3); the same condition exists in *D. colonnelloi* (Ayarzagüena 1985, fig. 3).

The osteological description is based on high-resolution tomographs of the skeleton of KU 315000, and comparisons are made with tomographs of other Terrarana. These were scanned on the OMNI-X high-resolution x-ray CT scanner at the Center for Quantitative Imaging at Pennsylvania State University at voxel dimensions of 0.03–0.05 mm. CT images and animations of the specimens presented here are available at DigiMorph (http://digimorph.org/). Terminology for the cranial osteology follows Trueb (1993). Proportions are based on measurements that were made from the tomograph with the measuring tool in Adobe Photoshop® Version 10.0. Except where noted, osteological measurements are those defined by Trueb (1977).

There is a notable discrepancy in the numbering of the digits in the hand. The description of external features of the hand follows the standard practice of the median (preaxial) digit ("thumb") being designated Finger I. Alberch and Gale (1985) and Fabrezi and Alberch (1996) showed that during development the first (preaxial) digit is lost, so that the first digit ("thumb") of anurans actually is Digit II. This arrangement is becoming standard in osteological studies. Consequently, in the description of external features, the digits on the hand are referred to as Fingers I, II, III, and IV; the same digits in the osteological description are designated Digits II, III, IV, and V.

Molecular analyses. We sequenced or obtained from GenBank data from 11 nuclear and six mitochondrial genes totaling 10,739 bases, for exemplars of 39 nobleobatrachian and four outgroup taxa, as well as three samples of the new family (Appendix 1). The nuclear genes were 28S ribosomal RNA (28S), cellular myelocytomatosis (c-myc), chemokine receptor 4 (CXCR4), histone H3 (HH3), sodium-calcium exchanger 1 (NCX1), proopiomelanocortin A (POMC), recombination activating protein 1 (RAG-1), rhodopsin (Rho), seventh in absentia (SIA), solute carrier family 8 member 3 (SLC8a3), and tyrosinase precursor (Tyr). The mitochondrial genes were 12S ribosomal RNA (12S), tRNA-Valine (tRNAV), 16S ribosomal RNA (16S), tRNA-Leucine (tRNAL), NADH dehydrogenase 1 (ND1), and cytochrome b (CytB). Most taxa are chimeric, consisting of sequences from several species within a genus or, in cases where sequences of congeners were not available, between closely related genera. Species composition of the chimeric sequences was guided by the results of previous molecular phylogenetic analyses (Frost *et al.* 2006; Wiens *et al.* 2005; Faivovich *et al.* 2005; Grant *et al.* 2007; Darst and Cannatella 2004; Guayasamin *et al.* 2008; Roelants *et al.* 2007). All nobleobatrachian families (sensu Frost 2009: Aromobatidae, Brachycephalidae, Bufonidae, Centrolenidae, Ceratophryidae, Craugastoridae, Cycloramphidae, Dendrobatidae, Eleutherodactylidae, Hemiphractidae, Hylidae, Hylodidae, Leiuperidae, Leptodactylidae, Strabomantidae) were represented, as well as multiple taxa of the most diverse families, or those families rendered polyphyletic in previous molecular phylogenetic studies of nobleobatrachians (Darst & Cannatella 2004; Faivovich *et al.* 2005; Frost *et al.* 2006; Grant *et al.* 2006; Roelants *et al.* 2007). The four outgroups included ranid, limnodynastid, myobatrachid, and *Calyptocephallela* sequences, representing the closest families outside Nobleobatrachia.

For specimens sequenced in this study (Appendix 1), genomic DNA was extracted from frozen or ethanol-preserved tissue samples using a Qiagen DNeasy Blood and Tissue kit. Polymerase chain reactions were performed at 50 μL volume using AmpliTaq DNA polymerase and ThermoPol buffer (NEB). Primer sequences were obtained from the literature (Biju & Bossuyt 2003; Bossuyt & Milinkovitch 2000; Faivovich

et al. 2005; Frost *et al.* 2006; Heinicke *et al.* 2007; Roelants & Bossuyt 2005; Roelants *et al.* 2007; Wiens *et al.* 2005). Standard reaction conditions were initial denaturation at 94° C (5 m), followed by 40 cycles of 94° C (30 s), 55° C (30 s), 72° C (60 s), and a final extension at 72° C (7 m). For some poor-yielding samples, annealing temperature was dropped from 55° C to 50° C or 46° C, and the duration of the annealing step was increased to 45 s. Amplified PCR products were purified via gel filtration or vacuum filtration (Millipore). Cycle sequencing was performed in forward and reverse directions for all samples, at the Pennsylvania State University Nucleic Acids Facility.

Newly generated sequences (GenBank accession numbers GQ345132–GQ345340) were combined with those obtained from GenBank (Appendix 2) and aligned using MUSCLE 3.6 under default parameters (Edgar 2004). Protein coding sequences were adjusted manually so that gaps corresponded with codon insertions or deletions. No premature stop codons were detected. 12S, 16S, and 28S ribosomal RNA alignments were refined based on structure models of *Eleutherodactylus riparius* Estrada and Hedges (Y10944) and *Xenopus laevis* (Daudin) (X02995) from the European ribosomal RNA database, using RNAsalsa 0.7.4 (Stocsits 2009) under default parameters. Poorly conserved loop regions of the ribosomal gene alignments were identified and excluded using Gblocks 0.91b (Castresana 2000) and the following parameters: maximum number of contiguous nonconserved regions (4), minimum length of a block (6), allowed gap positions (with half), and other parameters at default values. Third positions within codons of the mitochondrial ND1 and cytochrome b genes showed strong evidence of saturation when plots of transitions and transversions vs. genetic distance were made in DAMBE 5.0.25 (Xia & Xie 2001) and were excluded from the alignment to avoid biasing the non-model based analyses. For some taxa and genes, data were not available or could not be sequenced and were coded as missing data (Appendix 2). Single-gene neighbor-joining trees were produced to verify the presence of no strongly conflicting gene trees before concatenation of the genes into the final alignment. The final alignment includes 2,379 bases of mitochondrial structural RNA genes, 798 bases of mitochondrial protein-coding genes, 662 bases of nuclear structural RNA genes, and 6,900 bases of nuclear protein-coding genes.

In addition to this complete dataset, a shorter alignment was constructed without chimeric taxa, except one terminal that includes sequences of the former conspecifics *Thoropa miliaris* (Spix) and *T. taophora* (Miranda-Ribeiro). This reduced dataset includes sequences of the mitochondrial 12S, 16S, tRNAV, tRNAL, and ND1 genes, and the nuclear CXCR4, NCX1, RAG-1, and SLC8a3 genes, totaling 2,379 bases of mitochondrial structural RNA genes, 542 bases of mitochondrial protein-coding genes, and 3,631 bases of nuclear protein-coding genes. Both alignments have been deposited in TreeBASE, with accession number SN4553.

Molecular phylogenetic analyses were performed on both alignments using maximum likelihood (ML), Bayesian, and maximum parsimony (MP) methods, implemented in RAxML-VI-HPC 2.2.1, MrBayes 3.1.2, and MEGA 4.0, respectively (Stamatakis 2006; Huelsenbeck & Ronquist 2001; Tamura *et al.* 2007). For ML and Bayesian analyses, the nucleotide sequence data were divided into four partitions based on gene location (nuclear or mitochondrial genome) and type (structural RNA or protein-coding genes), with all parameters unlinked across these partitions. Alignment gaps were treated as missing data. In both cases, the best-fitting evolutionary model was identified as GTR + I + Γ under the Akaike information criterion using the program Modeltest 3.7 (Posada & Crandall 1998; Posada & Buckley 2004). For Bayesian analyses, this model was chosen. Because RAxML does not implement models with invariant sites, the GTR + gamma model was used for ML analyses. For the ML analyses, 100 independent searches were performed on the original dataset, and branch support was assessed for the most likely tree of these 100 runs with nonparametric bootstrapping (2,000 replicates). The Bayesian analyses were performed as two parallel runs for 15,000,000 or 20,000,000 generations, sampled every 500 generations. Each run employed three heated and one cold chain, with a temperature parameter of 0.25. The first 25% of samples were discarded as burnin. Convergence was assessed by the standard deviation of split frequencies (< 0.01 in all cases), potential scale reduction factors (approaching 1 for all parameters), and estimated sample sizes of parameters, using Tracer 1.3 (Rambaut & Drummond 2005) (> 100 for all parameters in each independent run across all partitions). Branch support was

assessed with posterior probabilities. For the MP analyses, close neighbor interchange searches were implemented, and 2,000 bootstrap replicates were run to provide branch support values.

A timescale of nobleobatrachian evolution was estimated using the topology from the ML analysis of the full dataset, but with the reduced alignment to avoid timing with chimeric taxa, and a Bayesian relaxed-clock model implemented in the T3 version of Multidivtime (Thorne & Kishino 2002; Yang & Yoder 2003). For comparative purposes, analyses were also performed on the same topology with the full alignment, and using the ML topology obtained using the reduced dataset (with the reduced alignment). The same partitions employed in phylogenetic analyses were also used in timetree estimation.

A total of five minimum and one maximum constraint were used as calibrations. The minimum divergence time between *Eleutherodactylus* and *Diasporus* was set at 15 million years ago (Ma), based on an amber-preserved *Eleutherodactylus* from Hispaniola (Iturralde-Vinent & MacPhee 1996; Poinar & Cannatella 1987). The minimum divergence time between the two members of *Bufo* sensu lato (*Rhinella* and *Duttaphrynus*) and *Melanophryniscus* was set at 24 Ma, based on fossil remains of "*Bufo*" from the Salla Beds of Bolivia (Báez & Nicoli 2004). Remains of *Hyla* from the Miocene of Austria set the minimum divergence time between *Hyla* and *Acris* at 16 Ma (Sanchiz 1998). Fossil evidence of *Calyptocephalella* dates to 61 Ma, setting the minimum divergence between it and myobatrachids (Báez 2000). The divergence time between *Litoria* and *Phyllomedusa* was constrained between 35 and 70 Ma, based on the timeframe when Australian hylids (represented by *Litoria*) could disperse from South America through Antarctica (Li & Powell 2001; Sanmartin & Ronquist 2004; Springer *et al.* 1998; Woodburne & Case 1996). Analyses were also performed with single calibrations removed, to gauge the relative effects of each calibration on the obtained divergence times.

For the analyses, priors of several other parameters are required, with some settings recommended by the creators of the software. The prior for root-to-tip age, rttm, was set at 145 (with 1 time unit equaling 1 million years), and its standard deviation at 40, based on recent molecular estimates of the divergence times between nobleobatrachians and myobatrachids (Roelants *et al.* 2007; Wiens *et al.* 2007). The rate prior, rtrate, was set at 0.0017, which is approximately the value of a root-to-tip branch length divided by the rttm. The standard deviation for rtrate was also set to 0.0017. The parameters brownmean and brownsd were set at 0.007, based on the recommendation that these values should be approximately 1 or 2 divided by rttm. Bigtime was set at 300. All other parameters (minab, newk, othk, thek) were maintained at default values. The analyses were run for 1,100,000 generations, with sampling every 100 generations and a burnin of 100,000 generations.

Results

Systematic accounts

Terrarana Hedges, Duellman, & Heinicke 2008

Definition. Species in this taxon have terrestrial breeding, direct development of terrestrial eggs (ovoviviparity in *Eleutherodactylus jasperi*), and embryonic egg teeth. All have arciferal (or pseudofirmisternal in a few taxa) pectoral girdles and partially fused calcanea and astragali; they lack Bidder's organs and intercalary elements in the digits. The majority have T-shaped terminal phalanges, and that is considered the ancestral condition (see below). The species range in SVL from 10–11 mm in female *Brachycephalus didactylus* and *Eleutherodactylus* (*Euhyas*) *iberia* to 110 mm in female *Craugastor pelorus*.

Content. This unranked taxon contains five families (914 species): Brachycephalidae, Ceuthomantidae n. fam. (see below), Craugastoridae, Eleutherodactylidae, and Strabomantidae.

Remarks. Dubois (2009) has objected to the spelling of the name Terrarana, proposing that it should be emended to "Terraranae" or "Terranae." His reasoning is that by doing so it would conform with his own rules of zoological nomenclature (See Dubois 2009, and references therein). In this case, it would change the name

from a noun in the nominative singular to one in the nominative plural, and thus be consistent with most higher-level names. His suggestion of "Terranae" was because he thought it would be easier to pronounce. However, these proposed changes are not supported by the Code of Zoological Nomenclature and therefore we do not support them.

As conceded by Dubois (2009), the name Terrarana could be considered a noun in the nominative plural if it were derived from the neuter noun *terraranum*. Moreover, other higher-level taxa of amphibians that end in the letter "A" are nouns in the nominative plural. Therefore, the name Terrarana, by itself, does not imply that it is a noun in the nominative singular or otherwise is inconsistent with the rules defined by Dubois (2009) for coining higher-level names. It was only the etymology given by Hedges *et al.* (2008) that created a potential conflict with Dubois' rules. To resolve that conflict, without changing the name, we propose here that that the neuter derivation of the name be assumed and that Terrarana be considered henceforth as a noun in the nominative plural. We reiterate, however, that the construction and use of such higher-level names is not regulated by the Code.

Ceuthomantidae new family

Type genus. *Ceuthomantis* Heinicke, Duellman, Trueb, Means, MacCulloch, and Hedges, 2009.

Diagnosis. A member of Terrarana (Hedges *et al.* 2008) based on direct development of terrestrial eggs (inferred), T-shaped terminal phalanges, "S" condition of adductor musculature as defined by Lynch (1986), and its lacking intercalary elements. It differs from other families in that group in having paired dorsal gland-like protrusions of unknown function in the post-temporal, and sacral regions. Although these protrusions appear to have contained lipids, they are not true glands. Body glands, similar in external appearance to these structures, are present in some species of *Eleutherodactylus* (Eleutherodactylidae) but they are located in the inguinal and flank regions. Also, computed tomography scans of the holotype show that the neurocranium is extraordinarily poorly ossified, and the neopalatine is unusually massive.

Content. One genus, *Ceuthomantis.*

Distribution. Known only from the Guiana Highlands, northeastern South America.

Ceuthomantis new genus

Type species. *Ceuthomantis smaragdinus* Heinicke, Duellman, Trueb, Means, MacCulloch, and Hedges, 2009.

Diagnosis. Same as for family. Members of the genus *Ceuthomantis* are unique compared to the strabomantid genera *Dischidodactylus* and *Pristimantis* in the Guiana Highlands by having notched digital discs on the fingers and toes and by lacking dentigerous processes of vomers.

Content. Tentatively three species, *C. aracamuni* (Barrio Amorós & Molina) and *C. caveribardus* (Myers & Donnelly), new combinations, plus *C. smaragdinus* n. sp. described below, are assigned to the genus.

Distribution. The genus is known only from elevations of 493–1540 m in the southern and eastern parts of the Guiana Highlands. These include Mt. Ayanganna and the Wokomung Massif in Guyana, Cerro Aracamuni and Sierra Tapirapecó in the Cerro Neblina Massif on the Venezuela-Brazil border, and possibly Sarisariñama Tepui in southern Venezuela (see Remarks). The species are known from the slopes of the mountains and the tops of tepuis.

Etymology. The generic name is masculine and derived from the Greek noun *mantis,* meaning treefrog and the Greek adjective *keuthos,* meaning hidden and alludes to its hidden existence in the tepuis of the Guiana Shield, which became known as the *Lost World* through the writings of Arthur Conan Doyle (1912).
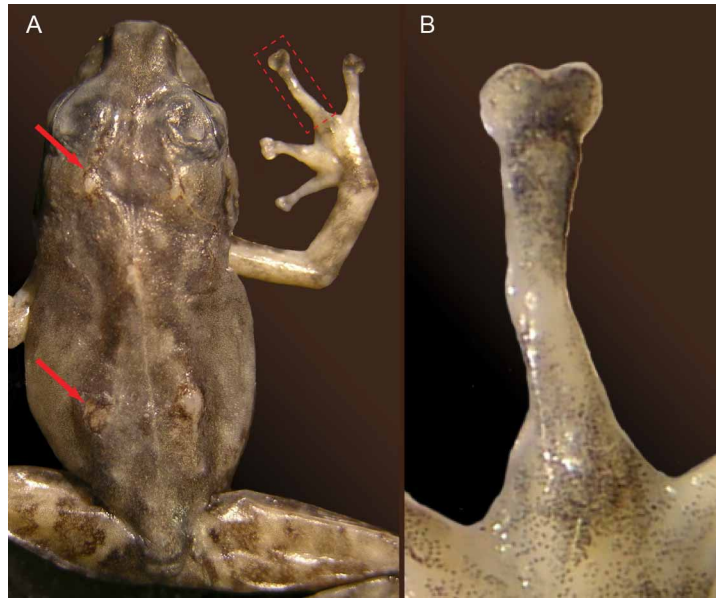
FIGURE 1. Dorsal view of female paratype of *Ceuthomantis smaragdinus,* KU 315000 SVL 19.5 mm. Arrows point to the dorsal glandlike structures. The third finger of the right hand is enlarged to show the notched anterior margin of the disc. Photographs by A. Campbell.

Ceuthomantis smaragdinus new species

Holotype. KU 300000, an adult male, from top of Kamana Falls on Mt. Kopinang, part of the Wokomung Massif, Potaro-Siparuni District, Guyana (05°00'08" N, 59°52'47" W, ~1540 m elevation), obtained on 18 July 2007 by D. Bruce Means. Field number CPI 10559.

Paratype. KU 315000, a subadult female collected with the holotype.

Referred specimen. ROM 40161, a juvenile, from Mt. Ayanganna, Potaro-Siparuni District, Guyana, 1490 m (05°24' N 59°57' W, 1490 m elevation), obtained on 20 October 2000 by Amy Lathrop and Carter Cox.

Diagnosis. This small frog has: (1) skin on dorsum smooth, that on belly areolate; dorsolateral folds absent; pair of dorsal protrusions in sacral region and small pair in scapular region; discoidal fold not evident; (2) tympanic membrane differentiated; tympanic annulus low, smooth, round, its diameter about 40% length of eye; (3) snout rounded in dorsal view, bluntly rounded in profile; (4) upper eyelid bearing prominent subconical tubercle; width of eyelid slightly less than interorbital distance; cranial crests absent; (5) dentigerous processes of vomers absent; (6) vocal slits present; nuptial excrescences absent; (7) Finger I shorter than Finger II; discs on outer fingers broadly expanded with terminal notch; (8) fingers lacking lateral fringes; (9) ulnar tubercles absent; (10) heel bearing prominent subconical tubercle; row of conical tubercles on outer edge of tarsus; (11) inner metatarsal tubercle elliptical 3x subconical outer metatarsal tubercle; plantar supernumerary tubercles absent; (12) toes lacking lateral fringes; webbing absent; Toe V slightly longer than Toe III; discs about same size as those on fingers; (13) dorsum olive brown with diffuse black markings and prominent bright green (in life) interorbital bar, subcanthal stripe, and diagonal bars in scapular region; venter pale gray with black mottling; (14) SVL in one male 19.8 mm, in one subadult female 19.5 mm.

Ceuthomantis smaragdinus shares a unique combination of five characters with two other species from elevated areas of the Guiana Shield that we tentatively place in *Ceuthomantis*: *C. aracamuni* and *C. cavernibardus*. These characters are notched digital discs, narrow heads, green coloration, and the absence of vomerine teeth and nuptial pads (Barrio-Amorós & Molina 2006; Myers & Donnelly 1997). Separately, each of these characters is found in other species of terraranans (Hedges *et al.* 2008; Lynch 1979; Lynch &

Duellman 1997; Duellman & Pramuk 1999), but their combination in species from the same region suggests a close relationship. Nonetheless, *C. smaragdinus* differs from both in having paired dorsal gland-like protrusions, prominent subconical tubercle on the upper eyelid and the heel, and a row of conical tubercles on the outer edge of the tarsus.

Other terraranans known from the highlands in the southwestern part of the Guiana Highlands are *Pristimantis avius* (Myers & Donnelly 1997) and *P. memorans* (Myers & Donnelly 1997). These, like all other *Pristimantis* known from the highlands, have vomerine teeth and both lack tubercles of the heels. Furthermore, *P. avius* differs from *C. smaragdinus* by having weak dorsolateral folds, marginate discs on the digits, no eyelid tubercle, a brown dorsum, and a pale orange or yellow venter. *Pristimantis memorans* differs from *C. smaragdinus* by having small tubercles on the eyelid, shallowly indented digital discs, a brown dorsum with dark brown markings, and a gray venter.

Description of the holotype. Small frog with head much longer than wide, head length 40.9% SVL, head width 33.3% SVL; head narrower than body; snout moderately long, rounded in dorsal view (Fig. 1), bluntly rounded in profile; eye-nostril distance 80.0% length of eye; loreal region concave; nostrils barely protruding, directed laterally at level well behind anterior margin of lower lip; canthus rostralis slightly curved, rounded in section; lips rounded; width of upper eyelid 85.7% interorbital distance; side of head vertical. One rounded postrictal tubercle posteroventral to tympanum; supratympanic fold weak, barely obscuring posterodorsal edge of tympanum; tympanic membrane differentiated; tympanic annulus low, smooth, round, its diameter 40.0% length of eye; tympanum separated from eye by distance about twice diameter of tympanum.

Skin smooth on dorsum, weakly granular on throat, areolate on belly; discoidal fold not evident; cloacal sheath short, not bordered laterally by fold or tubercles. Prominent subconical tubercle on upper eyelid and heel; row of conical tubercles on outer edge of tarsus; inner tarsal fold absent; inner metatarsal tubercle ovoid, elliptical, three times size of subconical outer metatarsal tubercle; ulnar tubercles absent; thenar tubercle elliptical, slightly elevated, much larger that low, bifid palmar tubercle; plantar supernumerary tubercles absent; subarticular tubercles low, rounded; nuptial excrescences absent; pairs of what appear to be small glandular structures in the post-temporal and sacral regions (Fig. 1).

Finger I shorter than Finger II; Finger III very long; relative lengths of fingers: I < II < IV < III; discs on outer fingers broadly expanded, rounded with terminal notch (Fig. 1), lacking lateral fringes; circumferential grooves present; Toe V slightly longer than Toe III; Toe IV very long; discs on toes expanded, rounded with terminal notch, about equal in size to those on fingers; toes not webbed, lacking lateral fringes; relative lengths of toes: I < II < III < V < IV; tip of Toe V extending to base of penultimate subarticular tubercle of Toe IV; tip of Toe III extending to point midway between antepenultimate and penultimate subarticular tubercles on Toe IV. When hind limbs flexed perpendicular to axis of body, heels broadly overlap; shank 59.6% SVL; foot length 40.1% SVL.

Vocal slits and single, median, subgular vocal sac present; vocal slits extending from midlateral base of tongue to point about two-thirds distance to angle of jaw; tongue ovoid, broadest posteriorly, not notched behind, free posteriorly for nearly half of its length; choanae ovoid, not obscured by palatal shelf of maxillary; cranial crests and dentigerous processes of vomers absent.

In life, dorsum dull olive-brown with diffuse black markings on body; black transverse bars on limbs; black longitudinal stripe on inner surface of forearm; black labial bars; broad black canthal stripe; bright, almost phosphorescent green interorbital bar; pair of diagonal marks in scapular region; spot on anterior surfaces of upper arm; distinct green bar below black canthal stripe (Fig. 2A); dorsal surfaces of discs on fingers white; dorsal surfaces of toe pads creamy white with black suffusion in terminal notch; venter creamy gray, heavily mottled in black; throat nearly entirely black (Fig. 2B); belly mottled black and gray; iris greenish bronze heavily flecked with black.

In preservative, dorsum tan with irregular paravertebral marks extending from occiput to sacrum; bright green marks in life now pale gray; limbs tan with brown transverse bars; posterior surfaces of thighs brown; belly cream with irregular brown spots; throat black; ventral surfaces of hind limbs brown with cream spots; palmar and plantar surfaces black.
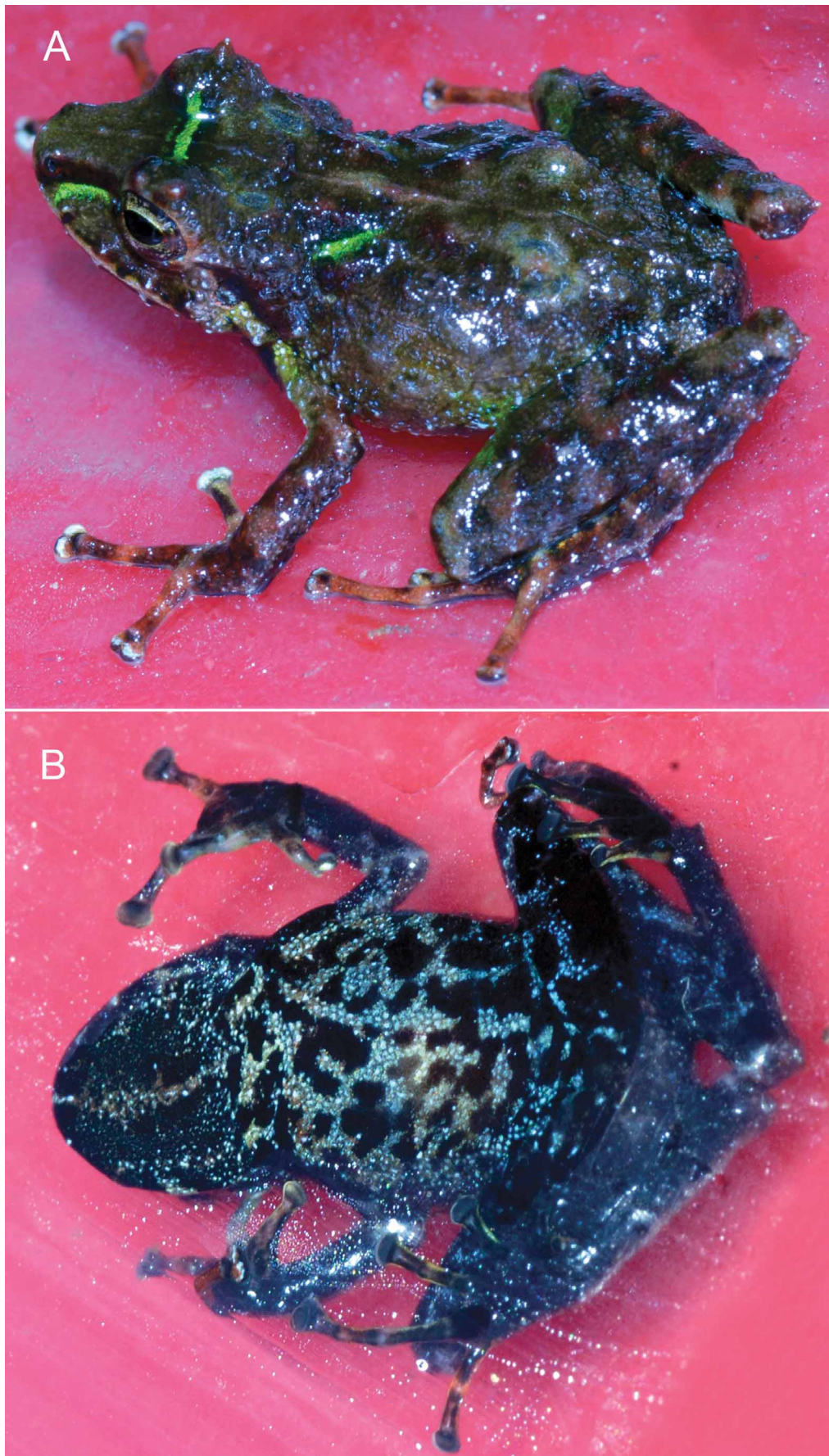
FIGURE 2. Dorsal (A) and ventral (B) views of the holotype of *Ceuthomantis smaragdinus* (KU 300000) in life. Photographs by D. B. Means.
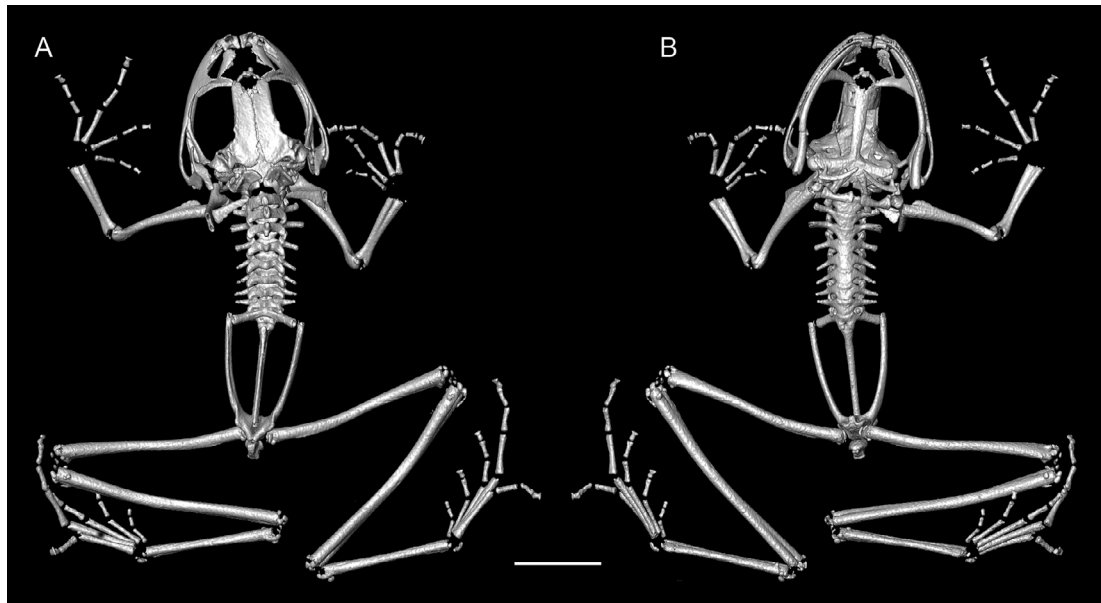
FIGURE 3. High-resolution tomographs of *Centhomantis smaragdinus,* KU 315000. A dorsal, B. ventral. Scale bar = 5 mm.

TABLE 1. Measurements and proportions of *Ceuthomantis smaragdinus.*

Character	KU 300000 (Male)	KU 315000 (Female)	ROM 40161 (Juvenile)
Snout-vent length	19.8	19.5	14.8
Shank length	11.8	11.7	8.2
Foot length	8.9	9.1	7.1
Head length	8.1	7.8	6.1
Head width	6.6	6.3	4.5
Interorbital distance	2.1	2.0	1.3
Eyelid width	1.8	1.8	1.1
Internarial distance	1.6	1.6	1.2
Eye length	2.5	2.4	2.0
Eye-nostril distance	2.0	1.9	1.5
Tympanum diameter	1.0	1.0	0.8
Head length/SVL	40.9%	40.0%	41.2%
Head width/SVL	33.3%	32.3%	30.4%
Eyelid/IOD	85.7%	90.0%	84.6%
Tympanum/Eye	40.0%	41.7%	40.0%
Shank/SVL	59.6%	60.0%	55.4%
Foot/SVL	40.1%	40.0%	47.9%

Measurements of holotype. Measurements and proportions of the three known specimens are given in Table 1.

Variation. Both adults (KU 300000 and 315000) and the one juvenile (ROM 40161) are alike structurally, except that glandlike protrusions are less pronounced in the juvenile. The dorsal color pattern is the same in all specimens; the bright green markings are distinct not only in adults but also in the juvenile. The throat in the female and in the juvenile are mottled like the belly, not black as in the male.

FIGURE 4. Distribution of the family Ceuthomantidae. Lowlands are indicated by green and uplands by brown. Known localities of the new family are indicated in the northeastern and southwestern portions of elevated areas on the Guiana Shield, in Venezuela, Brazil, and Guyana. (1) Mt. Kopinang, Guyana (*C. smaragdinus*, type locality), (2) Mt. Ayanganna, Guyana *C. smaragdinus*, referred specimen), (3) Pico Tamacuari, Venezuela and Brazil (*C. cavernibardus*), (4) Cerro Aracamuni, Venezuela (*C. aracamuni*), and (5) Sarisariñama Tepui, Venezuela (*C.* cf. *cavernibardus*).

The holotype (KU 300000) and female paratype (KU 315000) both bear what appear to be small glandular structures in the post-temporal and sacral regions (Fig. 1). Close examination reveals the skin to be slightly elevated and to lack melanophores. A section through the structure in KU 315000 shows a disassociation between the connective tissue and the overlying unpigmented skin, whereas the surrounding skin is loosely connected to the underlying muscles by the connective tissue. It is possible that the "bubble" of unpigmented skin might have been filled with adipose cells, which have dissolved in preservative.

Osteology. The head is widest anterior to angle of jaw at the level of the articulation of the quadratojugal and maxilla, at which level, the medial head length is 98% the head width. The overall width of the head diminishes gradually in the orbital region, being 86% of the greatest width (HWG of Trueb 1977) at the mid-

orbit level and 76% of this measure at the anterior margin of the orbit. The rostrum seems especially massive, with its medial length composing 25% of the length of the skull (HLM of Trueb 1977), and its posterior and anterior widths, composing 68% and 27%, respectively, of the greatest width of the skull (Fig. 3A).

The braincase is poorly ossified. Sphenethmoid ossification is limited to a narrow girdle of bone in the anterolateral walls of the braincase; the anterior limit of the bone is the orbitonasal canal, which has a complete margin in bone. There is an asymmetrical structure apparent dorsomedially that probably represents mineralization of ethmoidal cartilage. The prootic forms the bony anterior, anterodorsal, and anteroventral walls of the otic capsule; the bony posterior walls are formed by the exoccipital. These bones are so poorly ossified that epiotic eminences, as well as most of the lateral parts of the otic capsule, remain cartilaginous. The stapes are exceedingly delicate and small, but there is a large, bony operculum. The bony parts of the exoccipitals and prootics are widely separated from one another and their counter members.

The massive frontoparietals completely roof the central braincase from the anterior level of the orbit to the tectum synoticum posteriorly. The lamina perpendicularis is particularly well developed along the entire orbital margin of the frontoparietal. In the posterior part of the orbit, there is a small, knoblike orbital process on the frontoparietal. In lateral profile, a ventral process extends into the orbital fenestra from the lamina perpendicularis at the same level. Posterolaterally, the frontoparietal expands to form a flangelike process that extends dorsally along the anteromedial margin of the anterior epiotic eminence.

The parasphenoid floors the braincase (Fig. 3B). The long, narrow cultriform process extends from the anterior margin of the sphenethmoid to the otic capsules posteriorly. The alae completely floor the otic capsules and are approximately perpendicular to the cultriform process. The posteromedial process of the parasphenoid is broadly acuminate and does not reach the margin of the foramen magnum.

The nasal region is remarkable for its lack of bony armament. The small, slender nasals are broadly separated—apparently poised along the anterolateral margins of the olfactory capsules leaving the central portions of the capsules exposed in cartilage. Ventrally, the vomers are revealed as a pair of L-shaped bones that seem to lack a dorsal flange. The vomers seem to consist only of pre- and postchoanal bony process to support the internal choana. The paired septomaxillae are minute and lie dorsal to the partes palatinae and the articulation between the maxilla and premaxilla.

In contrast to the seemingly weak construction of the endocranium, the suspensory apparatus, maxillary arcade, and its support is robust. The otic and ventral rami of the squamosal are especially well developed, with the otic ramus seeming to extend along the entire lateral margin of the cartilaginous crista parotica. The zyogmatic ramus is short and acuiminate in lateral profile. The quadratojugal is particularly robust and bears a broadly overlapping articulation with the maxilla. The maxillae and premaxillae bear teeth, and both have moderately well developed partes palatinae; that of the premaxilla is medially notched to produce prominent medial and lateral flanges. The pars facialis of the maxilla is well developed and bears a large, acuminate preorbital process that extends nearly to the ventral margin of the nasal lateral to the planum antorbitale at the anterior margin of the eye. Anteriorly, the pars facialis overlaps the lateral margin of the pars dentalis of the premaxilla slightly. The pterygoid is a stout, triradiate element. The anterior ramus extends toward the braincase from the maxilla at the mid-orbit level and braces against the anteroventral margin of the otic capsule via the short medial ramus. The posterolateral ramus lies in the same plane as the anterior ramus and is about half its length; it provides support for the palatoquadrate cartilage and the jaw articulation. One of the most extraordinary features of the skull is the massive neopalatine, which seems to have encased completely the planum antorbitale and extends from the sphenethmoid laterally to the lingual margin of the maxilla.

The main component of the mandible is the stout angulosplenial, which is weakly sigmoid, bears scarcely no coronoid flange, and extends nearly to the mentomecklian bone anteriorly. The dentary is fused to the mentomecklian anteriorly and extends along the lateral surface of the mandible to terminate in the posterior part of the orbit. The only part of the hyoid revealed are the posteromedial processes, which are long, slender elements that are slightly expanded proximally and distally; the proximal expansion is slightly greater than the distal expansion. There is no mineralization in the hyoid corpus.

FIGURE 5. Habitat of *Ceuthomantis smaragdinus* at 1540 m on Mt. Kopinang, Guyana. The holotype was found about 5 m from the stream in the foreground in Figure 5A; the paratype was found on a leaf about 10 m away from the other side of the stream slightly to the left of the middle of Figure 5B. Photographs by D. B. Means.

The vertebral column is composed of eight nonimbricate, procoelous vertebrae. The atlantal cotylar arrangement is stalked and Type I of Lynch (1973). The tranverse processes are short and not expanded. There is little variation in the overall width of vertebrae with the vertebral profile being as follows: III > Sacrum > II > IV > VII > V $\cong$ VI > VIII > I. The neural arches are well developed and bear neural spines that are most prominent on Presacrals I–IV; however, the neural arches are exceedingly narrow, with the result that much of the spinal column is exposed dorsally. The short, round sacral diapophyses are nearly uniform in width and directly slightly posterolaterally. The sacrum has a bicondylar articulation with the urostyle. The urostyle is short, being only 84% of the length of the presacral vertebral column. It bears a well-developed dorsal crest and one pair of nerve foramina; there is no other evidence of postsacral vertebrae.

The pectoral girdle likely is arciferal. The clavicles are robust, curved, and moderately broadly separated from one another medially; the bones are separated from the adjacent scapulae and coracoids by cartilage. The posterior margin of the stout coracoid is straight, whereas the anterior margin is convex; the long axis of the

coracoid is nearly perpendicular to the longitudinal axis of the body. The glenoid and sternal ends of the coracoid are about equally expanded and slightly more than twice as wide as the midshaft width of the bone. A distinct notch separates the pars acromialis from the pars glenoidalis of the scapula, which is long and slender, with shallowly concave anterior and posterior margins. The suprascapular margin is about twice the width of the narrowest part of the bone, and the length is slightly more than three times the width of the suprascapular margin. The cleithrum is a dagger-shaped element; there is no indication of mineralization of the suprascapular cartilage. Ossified or mineralized pre- and postzonal elements are absent.
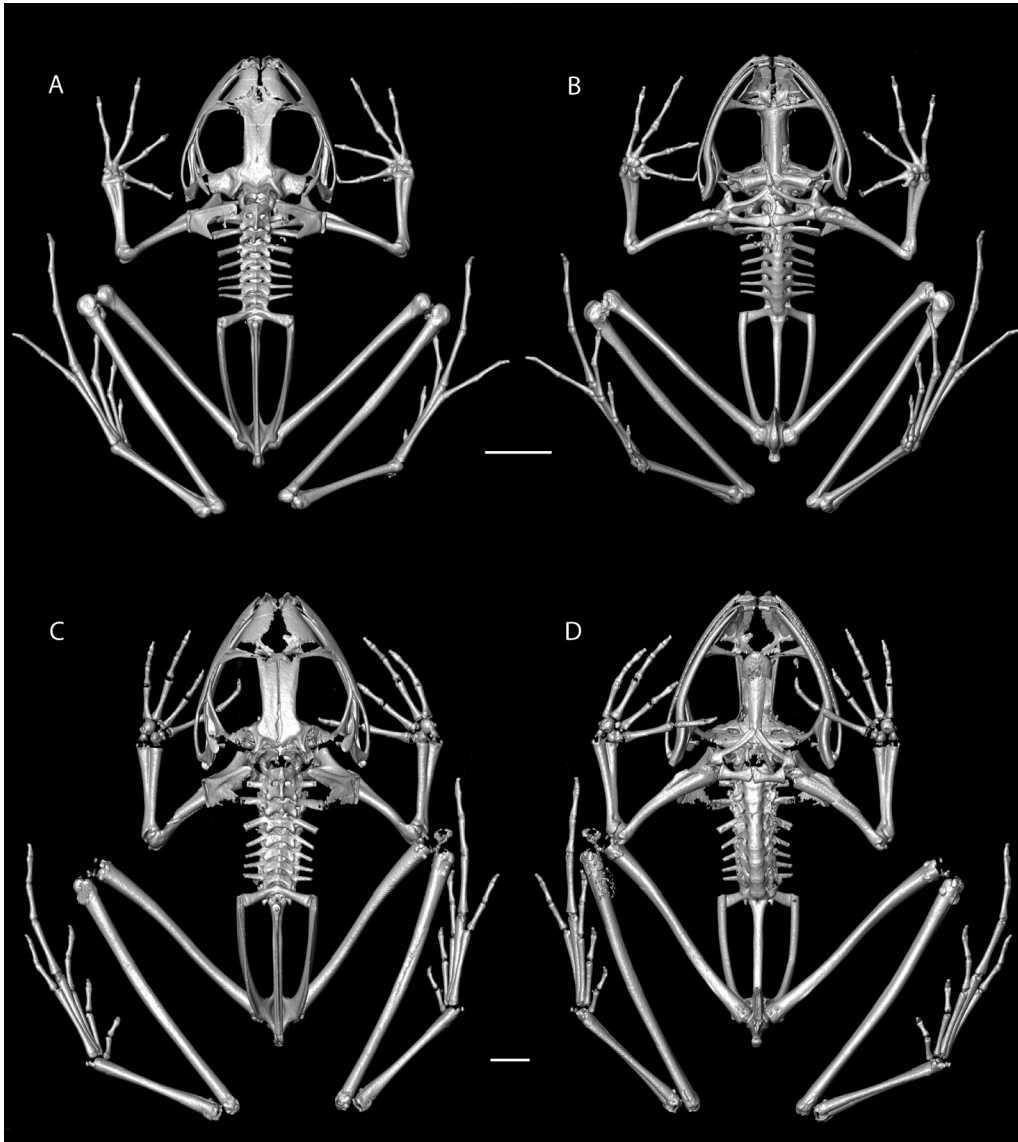
FIGURE 6. High-resolution tomographs of terraranan frogs representing two families (left, dorsal view; right, ventral view). (A–B) Brachycephalidae, *Ischnocnema guentheri* (KU 92816); (C–D) Craugastoridae, *Haddadus binotatus* (KU 92808). Scale bars = 5 mm.

The head of the humerus is cartilaginous. There is a moderate crista ventralis or deltoid crest extending along the proximal third of the bone. The cristae medialis and lateralis are not evident, but the eminentia capitata and ulnar and radial condyles are relatively well developed. The radio-ulna has a low olecranon and shallow sulcus intermedius; the epiphyses of the ulna and radius are cartilaginous. All carpal elements and the prepollex, if it is present, are cartilaginous.

The phalangeal formula is 2-2-3-3, and the relative lengths of the digits in increasing order is: II > III > V > IV. Concerning the phalangeal formula: fingers are numbered preaxially to postaxially from II–

V, in consistency with the hypothesis that Digit I was lost in anurans (Alberch & Gale 1985; Fabrezi & Alberch 1996; Shubin & Alberch 1986); the reader is cautioned that in older accounts, fingers are numbered from I to IV. The relative lengths of the metacarpals in increasing order is: II > V > III > IV. The phalangeal elements are well ossified with cartilaginous epiphyses. The terminal phalanges are stout, thick elements that are almost hourglass-shaped, with T-shaped distal ends (Fig. 1C–D).
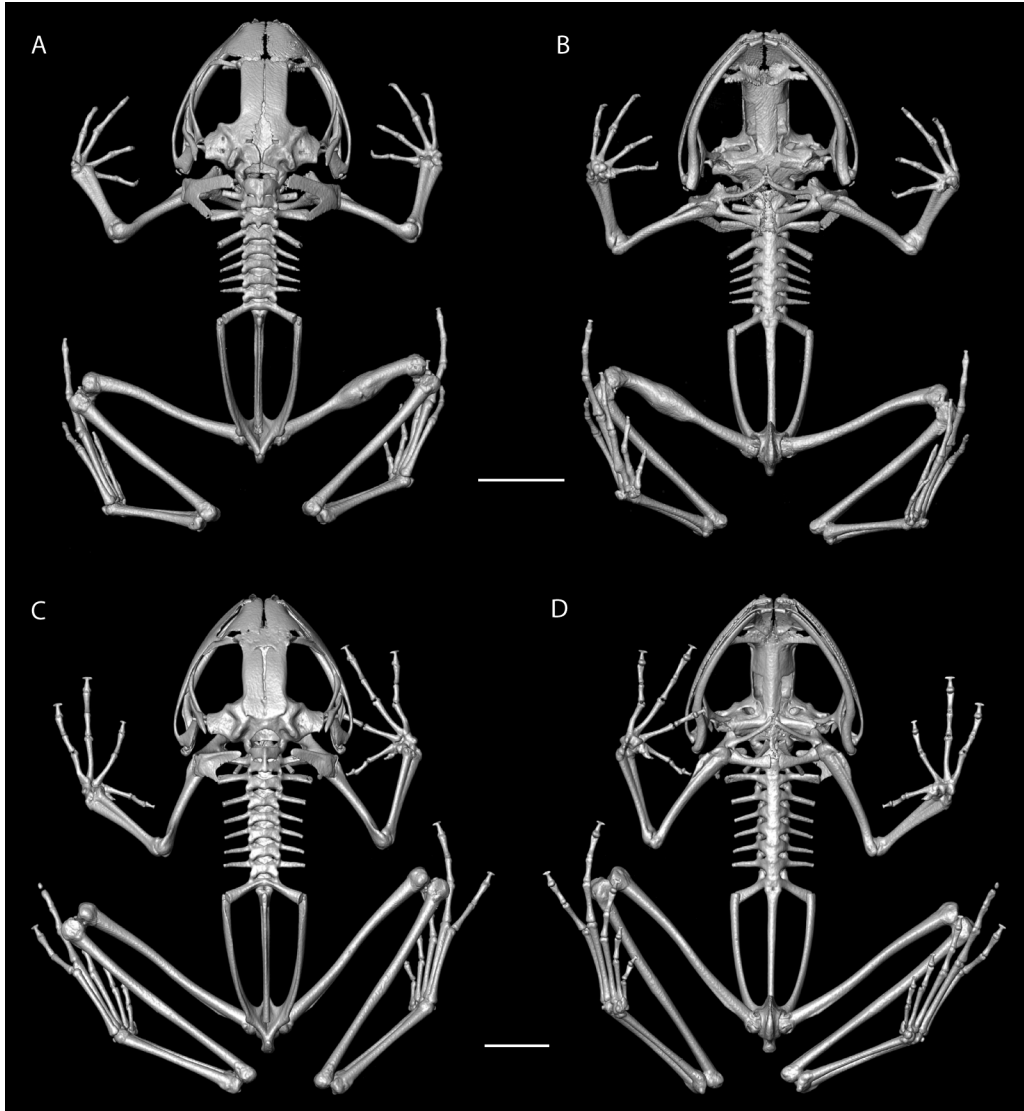
FIGURE 7. High-resolution tomographs of terraranan frogs representing two families (left, dorsal view; right, ventral view). (A–B) Eleutherodactylidae, *Eleutherodactylus gossei* (SBH 266440; and (C–D) Strabomantidae, *Pristimantis pulvinatus* (KU 166368). Scale bars = 5 mm.

The postsacral trunk region is short and narrow. The dorsal width of the pelvis at the sacrum is 57% of its overall length, and the angle of expansion is about 33˚. The internal margin of the pelvis in dorsal view describes a narrow U-shape. The ilial shaft is smooth and bears a scant indication of low, rounded dorsal ridge that terminates posteriorly in a low knob of a posterior prominence. The preacetabular angle is about 90˚. The pubes are lightly mineralized. The ischium is well ossified. The acetabulum is round; about two thirds of it is formed in bone by equal contributions of the ilium and ischium.

There is nothing particularly remarkable in the hind limb except for the lack of ossification (but presence of scattered mineralization) of the epiphyses of the femur, tibiofibula, and tibiale and fibulare. The tibiale and fibulare seem especially long, being about 58% of the length of the tibiofibula. Tarsal elements and a

prehallux, if present, are cartilaginous. The phalangeal formula is 2-2-3-4-3, and the relative lengths of the digits in increasing order is: I > II > III = V > IV. The relative lengths of the metacarpals in increasing order is: I > II > III = V > IV. The phalangeal elements are well ossified with cartilaginous epiphyses. The terminal phalanges are stout, thick elements that are almost hourglass-shaped, with T-shaped distal ends (Fig. 7C–D).

Distribution and ecology. *Ceuthomantis smaragdinus* is known from two of the easternmost mountains in the Guiana Shield, Mt. Ayanganna and Mt. Kopinang in the Wokomung Massif (Fig. 4). These mountains are separated by 37 km of uplands that support lower montane forest (Huber et al 1995). At the type locality, the forest consists of shrubs, including Melastomataceae (Myrtales), broad-leafed trees about 12 m high, and a few small tree ferns (Cyatheales); the trunks, boles, and limbs of all are festooned with epiphytes, especially dense olive-green moss and many bromeliads. The ground is deep organic peat covered with the same moss and bromeliads as on the trees. The holotype and paratype were collected after dark in cloud forest at an elevation of about 1540 m. The holotype was sitting on a leaf 1.5 m above the ground about 5 m from a cascading stream (Fig. 5A); another leaf sheltered it from a heavy rain. The paratype was found 30 min later during a light rain. It was perched on a leaf about 10 m away from the stream slightly to the left of the middle of Figure 5B. The juvenile from Mt. Ayanganna was collected at night amidst leaf litter on the ground in dense low-canopy forest at an elevation of 1490 m.

At the type locality 18 other species of anurans were found—*Oreophrynella* cf. *macconnelli* Boulenger, *Anomaloglossus beebei* (Noble), *A. kaiei* (Kok, Sambhu, Roopsind, Lenglet & Bourne), *Pristimantis saltissimus* Means and Savage, *P. dendrobatoides* Means and Savage, *Pristimantis* sp., *Leptodactylus lutzi* Heyer, *Stefania ayangannae* MacCulloch and Lathrop, *S. coxi* MacCulloch and Lathrop, *S. roraimae* Duellman and Hoogmoed, *Vitreorana gorzulae* (Ayarzagüena), *Hypsiboas sibleszi* (Rivero), *Myersiohyla kanaima* (Goin and Woodley), *Osteocephalus* cf. *cabrerai* (Cochran and Goin), *O.* cf. *exophthalmus* (Smith and Noonan), *Otophryne steyermarki* Rivero, and two species of "*Bufo.*" Only six of these are represented in the other 16 species that were found at 1490 m on Mt. Ayanganna—*Anomaloglossus beebei* (Noble), *A. tepuyensis* (La Marca), *Oreophrynella dendronastes* Lathrop and MacCulloch, *Stefania ackawaio* MacCulloch and Lathrop, *S. ayangannae* MacCulloch and Lathrop, *S. coxi* MacCulloch and Lathrop, *S. roraimae* Duellman and Hoogmoed, "*Hyla*" *warreni* Duellman and Hoogmoed, *Hypsiboas roraima* (Duellman and Hoogmoed), *Myersiohyla kanaima* (Goin and Woodley), *Osteocephalus phasmatus* MacCulloch and Lathrop, *Leptodactylus lutzi* Heyer, *Pristimantis inguinalis* (Parker), *P. jester* Means and Savage, *P. marmoratus* (Boulenger) and *P. pulvinatus* (Rivero).

Etymology. The specific name (*smaragdinus*) is a Latin adjective meaning emerald green and refers to the distinctive marks on the head and body.

Remarks. We refer *Pristimantis aracamuni* and *P. cavernibardus* to *Ceuthomantis* based on their sharing, with *Ceuthomantis smaragdinus*, a unique combination of five characters (cited above). However, we consider this arrangement to be tentative because genetic data are unavailable for either species and both lack the paired dorsal gland-like structures of *C. smaragdinus*. An unusual behavioral trait (for terraranans)—diurnal calling—may be shared by these three species. *Ceuthomantis aracamuni* were found during the day on moss and rocks in a small creek (Barrio-Amorós & Molina 2006), and *C. cavernibardus* were calling during the day in caves formed by granite boulders or on roots and moss (Myers & Donnelly 1997). At the type locality of *C. smaragdinus,* frogs of an unknown species (perhaps *C. smaragdinus*) were calling vociferously during the day from a site where a small stream emerged amongst large boulders. Barrio-Amoros and Brewer-Carias (2008) reported hearing *P.* cf. *cavernibardus* calling during rainy or cloudy days on Sarisariñama.

Barrio-Amorós and Brewer-Carías (2008) reported "*Pristimantis*" cf. *cavernibardus* from elevations of 1100–1375 m of Sarisariñama Tepui, which is about 380 km NNE of Cerro Aracamuni and Sierra Tapirapecó. Their color photograph (Fig. 13) shows a narrow nearly phosphorescent interorbital bar like that in *Ceuthomantis smaragdinus.* The tepuis in extreme southern Venezuela and in Guyana seem to harbor a biota that is distinct from the tepuis on the northern part of the Guiana Highlands in Venezuela (McDiarmid & Donnelly 2005).

Ceuthomantis cavernibardus has large, unpigmented eggs (Myers & Donnelly 1997); these are typical of direct-developing species of terraranans. The only female of *C. smaragdinus* is a subadult with small, unpigmented eggs in the ovaries. Consequently, direct development of terrestrial eggs on *C. smaragdinus* can only be assumed. Large, unpigmented eggs also are associated with frogs that have nonfeeding tadpoles, including hemiphractids (Duellman 2007; Wells 2007); consequently, additional data are needed to confirm the reproductive mode of *Ceuthomantis*.

Inasmuch as the osteological data for *Ceuthomantis smaragdinus* were obtained from a tomograph, the only direct comparisons are made with representatives of the other four families of Terrarana for which tomographs exist. These are *Ischnocnema guentheri* (Steindachner) of the Brachycephalidae, *Haddadus binotatus* (Spix) of the Craugastoridae, *Eleutherodactylus gossei* Dunn of the Eleutherodactylidae, and *Pristimantis pulvinatus* (Rivero) of the Strabomantidae (Figs. 6 and 7).

Comparison of the taxa reveals several rather striking differences. *Ischnocnema, Eleutherodactylus,* and *Pristimantis* have rather well-ossified skeletons in contrast to that of *C. smaragdinus*. As a result, note that the anterolateral part of the braincase is complete, although the sphenethmoid may be marginally ossified dorsally (*E. gossei*); likewise, the exoccipitals are synostotically united to one another and to the prootics so as to produce well-developed otic regions. The nasals are large; ventrally, vomers and robust pterygoids are present. The neural arches of Presacrals I and II are fused. The epiphyses of the long bones are uniformly mineralized and ossification of the carpal and tarsal elements is clearly evident.

The shape of the head (dorsal/ventral profiles) of *Ceuthomantis* is distinctly different from that of *Pristimantis, Ischnocnema,* and *Eleutherodactylus,* which one could reasonably interpret as being more "typical" of terraranans, with their broadly arced jaws and almost triangular heads. In contrast, the head of *Ceuthomantis,* with its narrow otic region and wide preorbital region, has an overall shape somewhat reminiscent of a quadrangular caudate skull. Note the disproportionately large rostrum in contrast to that of *Pristimantis,* and the shape of the mandible in ventral view; it is strongly sigmoid in *Ischnocnema, Eleutherodactylus,* and *Pristimantis,* and only weakly so in *Ceuthomantis*. The transverse processes of the presacral vertebrae of *Ceuthomantis* are much shorter than those of *Ischnocnema, Eleutherodactylus,* and *Pristimantis,* and the sacral diapophyses are less robustly developed. *Ceuthomantis* lacks well-developed preacetabular ilium, whereas *Ischnocnema, Eleutherodactylus, Haddadus,* and *Pristimantis* possesses distinct, well-developed preacetabular ilia. The terminal phalanges are small, knobby expansions in *Ischnocnema, Eleutherodactylus,* and *Haddadus,* whereas they are larger and have a distinctive hourglass shape in *Ceuthomantis* and a broadly expanded, gracile T-shape in *Pristimantis*.

Of the four genera and families available for comparison with *Ceuthomantis,* it bears a few features in common with the craugastorid, *Haddadus*. In *Haddadus binotatus,* the anterior braincase (sphenethmoid) is scarcely ossified and the otic capsule is very poorly developed. The neural arches of Presacrals I and II are not fused, and the transverse processes of the presacrals are short, resembling those of *Ceuthomantis*. Despite the reduced ossification of *Haddadus,* the carpal and tarsal elements are mineralized in contrast to those in *Ceuthomantis*.

There is a brief osteological description for one other species included in *Ceuthomantis, C. cavernibardus* (Myers & Donnelly 1997). The authors noted that in this species the skull is a "little wider than long," and that the nasals are "moderate, not in medial contact, well separated from frontoparietals by sphenethmoid." These comments suggest that *C. cavernibardus* has larger nasals and that the sphenethmoid is ossified dorsally, in contrast to *C. smaragdinus*. Likewise, *C. cavernibardus* has vomers, whereas *C. smaragdinus* lacks them. Both taxa have widely separated occipital condyles on short stalks, similar parasphenoids, squamosals, and pterygoids. Likewise, as described by Myers and Donnelly (1997), the configurations of the axial column, and pectoral and pelvic girdles seem to resemble one another; however, based on their comments about the tarsal elements and the skeleton in general, it is evident that the skeleton of *C. cavernibardus* is more completely ossified than is that of *C. smaragdinus*.

Phylogenetic Relationships of *Ceuthomantis*

In order to determine the relationships of Ceuthomantidae, we estimated a molecular phylogeny with sequences from 17 nuclear and mitochondrial genes and exemplars of all nobleobatrachian families. For both the full and limited alignments, all analyses support the position of the new family as the basal family of Terrarana, and support marsupial frogs (Hemiphractidae) as the closest relatives of Ceuthomantidae + Terrarana (Figs. 8–10). Support values are significant ($\geq 95\%$) for placement of the new family as the closest relative of, but outside the four terraranan families with both Bayesian analyses and the ML analysis of the complete dataset. The Terrarana + Ceuthomantidae + Hemiphractidae clade received significant support only from the Bayesian analysis of the full dataset, and moderate support from the ML analysis of the full dataset.

Individual gene trees (not shown) revealed no strongly conflicting phylogenetic signal. In general, the gene trees did not include enough data to resolve relationships among families, and only relationships within families received moderate (bootstrap > 70%) support. However, for most genes, the new family is recovered either as the closest relative of Terrarana or embedded in Terrarana.
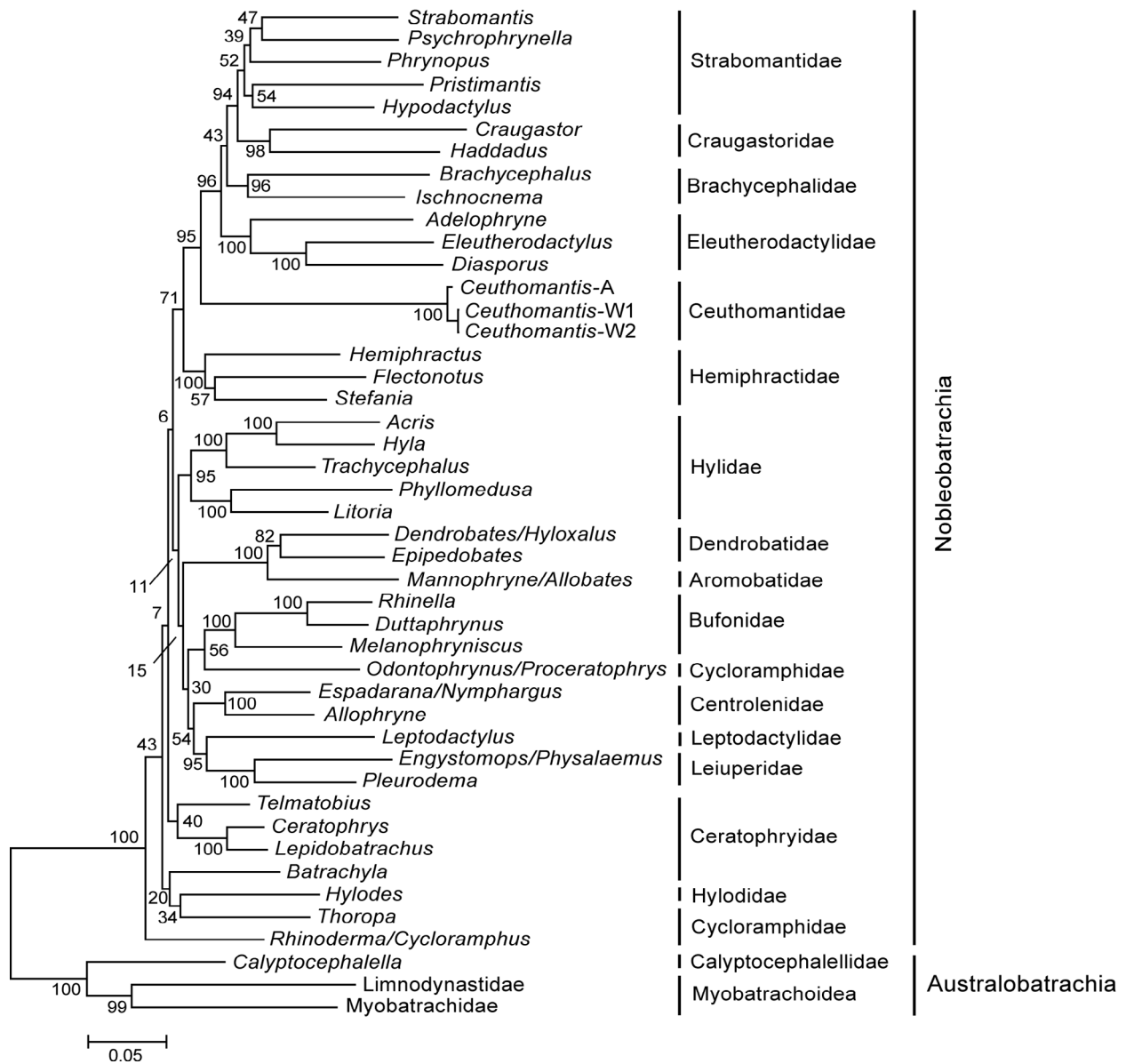
FIGURE 8. Maximum likelihood phylogeny of nobleobatrachian frogs represented by selected genera and constructed using sequences from 17 genes. The tree is rooted with Ranidae (not shown). Bootstrap support values are indicated at nodes. Higher classification is indicated to the right.
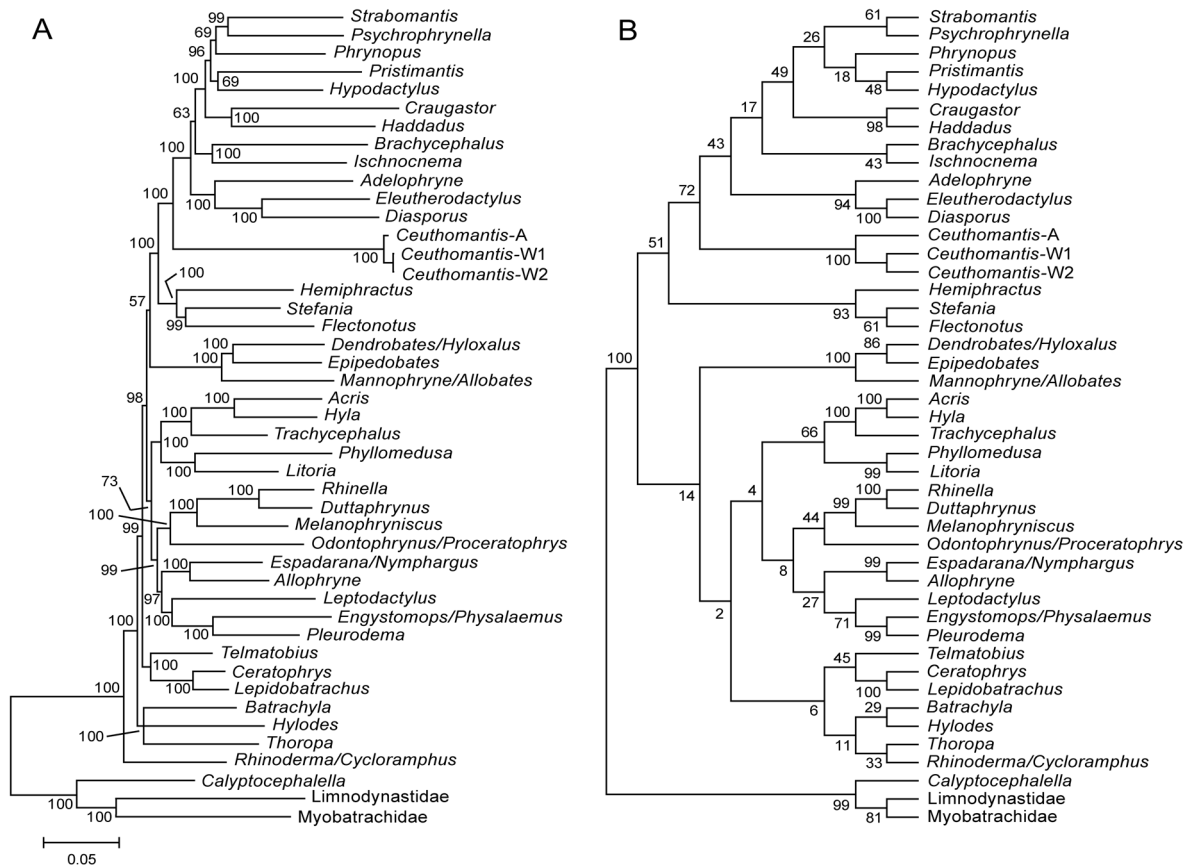
FIGURE 9. (A) Bayesian and (B) maximum parsimony phylogenies of nobleobatrachian frogs represented by selected genera and constructed using sequences from 17 genes. The trees are rooted with Ranidae (not shown). Support values (Bayesian posterior probabilities or MP bootstrap values) are indicated at nodes.

No evidence was found for the polyphyly of marsupial frogs (Faivovich *et al.* 2005; Frost *et al.* 2006; Wiens *et al.* 2005), consistent with some other recent analyses (Wiens *et al.* 2007; Guayasamin *et al.* 2008). Previous molecular phylogenetic analyses have identified various close relatives of Terrarana, including some or all hemiphractids (Faivovich *et al.* 2005; Wiens *et al.* 2005), and phyllomedusine + pelodryadine hylids (Roelants *et al.* 2007), or placed Terrarana outside most other nobleobatrachians (Darst & Cannatella 2004; Frost *et al.* 2006), but none of those proposed relationships had significant support. For example, Guayasamin *et al.* (2008) included four genera of hemiphractid frogs. They recovered a clade with significant support that included all marsupial frogs in the nuclear and complete phylogenies but not in the mitochondrial analysis; in all analyses terraranans were in a polytomy within Nobleobatrachia and not significantly linked to hemiphractids.

Within Terrarana, ML and Bayesian analyses strongly support Craugastoridae and Strabomantidae as closest relatives. Eleutherodactylidae is recovered as basal to Brachycephalidae, Craugastoridae, and Strabomantidae in all analyses, but with low support. Most relationships among other nobleobatrachian families remain unresolved. The major exception is the significantly supported close relationship between Leptodactylidae and Leiuperidae (removed from Leptodactylidae by Grant *et al.*, 2006), which has been recovered with non-significant support in other studies (Darst & Cannatella 2004; Faivovich *et al.* 2005; Frost *et al.* 2006; Roelants *et al.* 2007). Conversely, two other former components of Leptodactylidae, Ceratophryidae and Cycloramphidae, are rendered polyphyletic in all analyses.

The results of the molecular phylogenetic analyses (Figs. 8–10) are largely compatible with recent hypotheses regarding overall terraranan relationships and evolution (Heinicke *et al.* 2007; Hedges *et al.*

2008). The four previously-named families—Brachycephalidae, Craugastoridae, Eleutherodactylidae, and Strabomantidae—were each found to be monophyletic, with all but Strabomantinae receiving significant support. However, the lone representative of the strabomantid subfamily Holoadeninae (*Psychrophrynella*) is embedded among the four exemplars of Strabomantinae, a subfamily that received only poor support previously (Hedges *et al.* 2008). Considering the limited sampling of strabomantids in this study, any revision of the content of the strabomantid subfamilies must await future analyses with more taxa. Previous studies have suggested that West Indian *Eleutherodactylus* and Middle American *Craugastor* originated via dispersal from South America (Lynch 1971; Hedges *et al.* 1989; Crawford & Smith 2005; Heinicke *et al.* 2007). The discovery of the basal terraranan, *Ceuthomantis*, reinforces a South American origin for Terrarana as a whole, whereas a strabomantid + craugastorid clade supports separate origins of terraranans in Middle America and the West Indies.
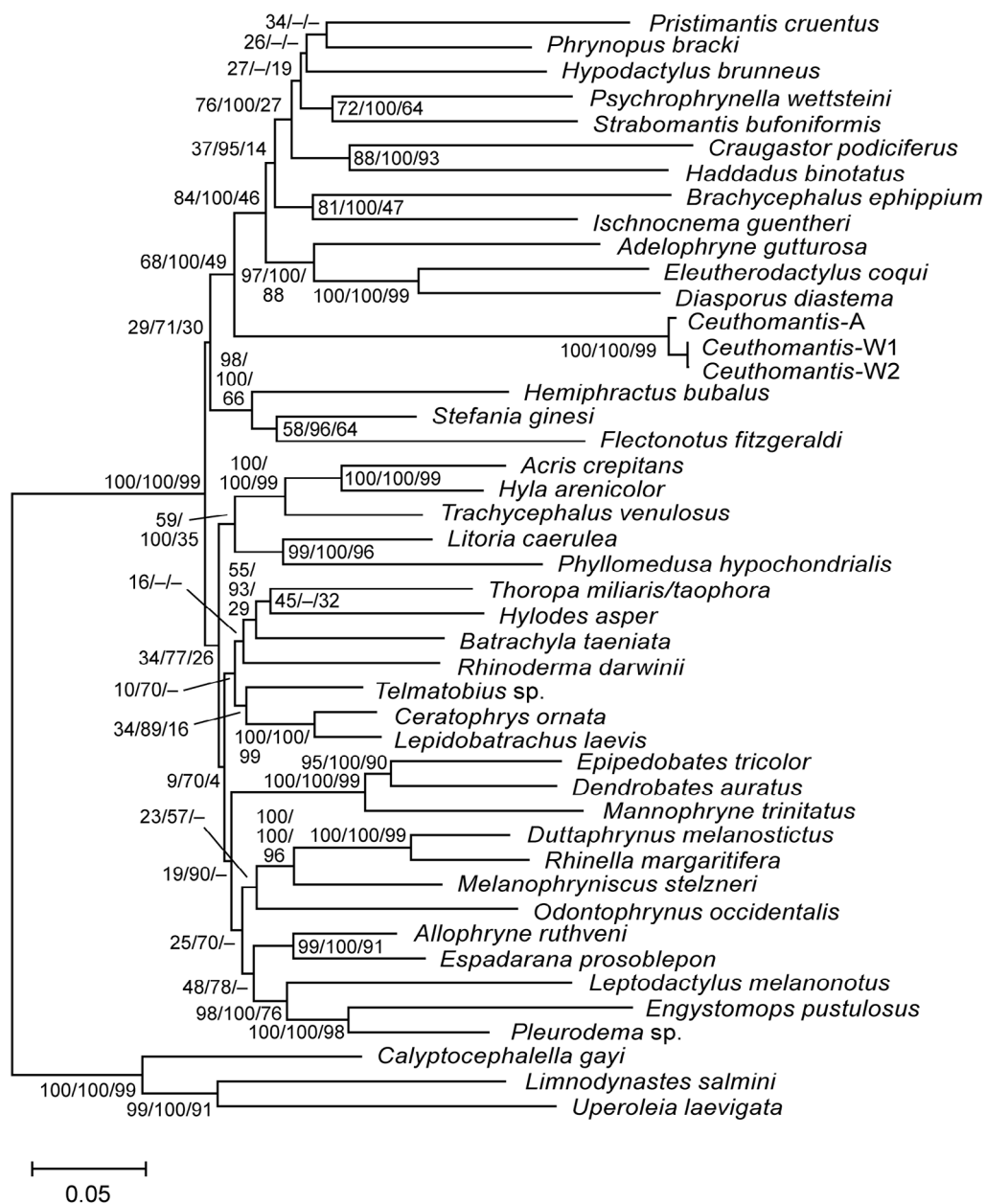
FIGURE 10. Phylogeny of nobleobatrachian frogs represented by selected species and constructed using sequences from 9 genes. The tree is rooted with *Rana temporaria* (not shown). Support values (ML bootstrap/Bayesian posterior probability/MP bootstrap) are indicated at nodes. Bayesian and MP support values are not given in cases where those phylogenies conflicted with the ML phylogeny.
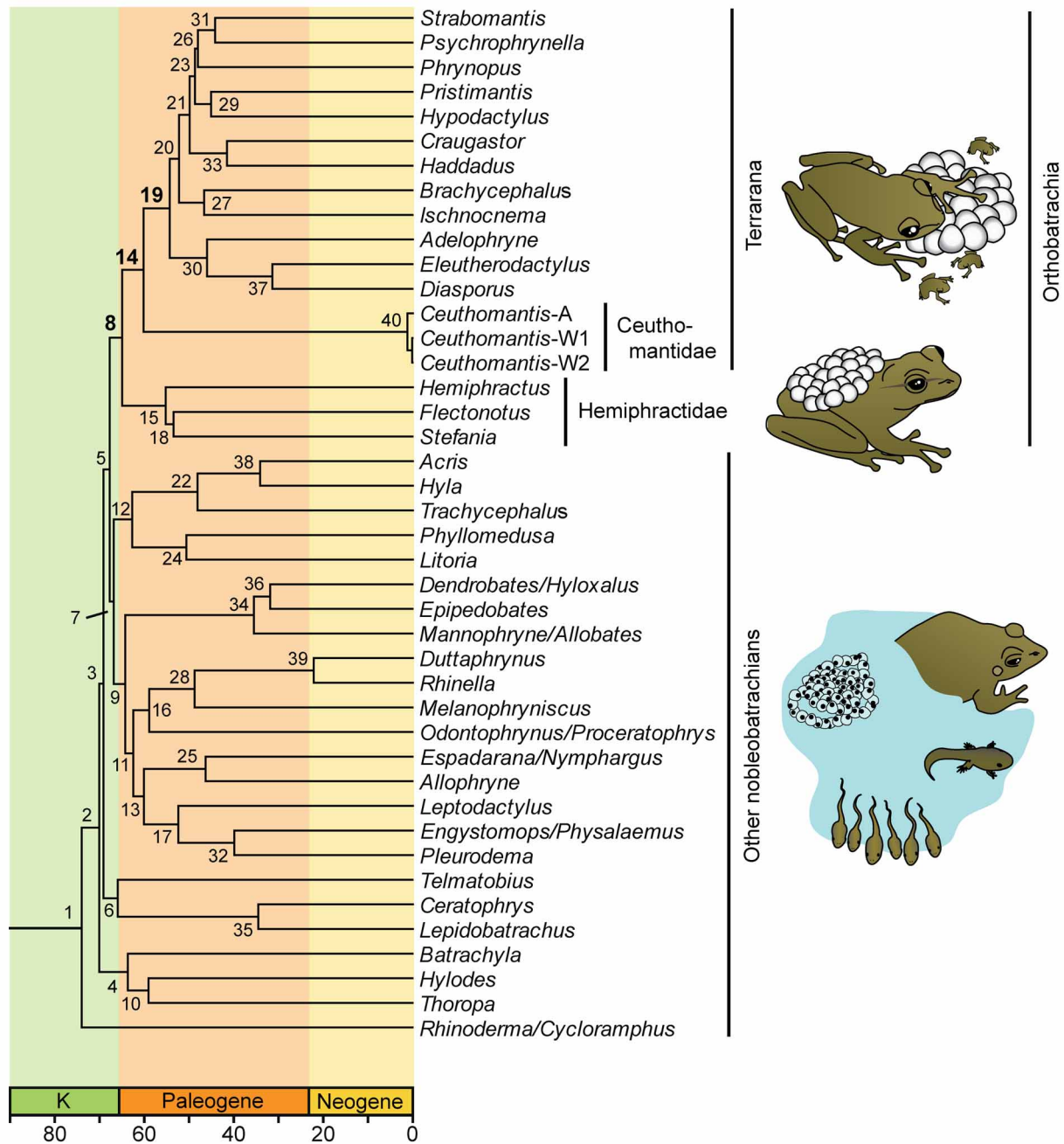
FIGURE 11. Timetree of nobleobatrachian frogs represented by selected genera and estimated with a Bayesian analysis of sequences from 9 genes, based on a topology obtained from the ML analysis of 17 genes (Figure 8). Numbers on nodes refer to time estimates and credibility intervals of time estimates (Table 2); those in bold are nodes discussed in the text. Illustrations portray the major reproductive modes of the genera and families, with most direct-developing species (i.e., no aquatic larvae) contained in Terrarana (Ceuthomantidae and four other families) that nearly always lay eggs on substrate, and Hemiphractidae that carry their eggs on their backs. Nearly all other nobleobatrachians have aquatic larvae (e.g., tadpoles).

Times of divergence within Terrarana (Fig. 11, Table 2) are similar among all analyses. Multiple repeated runs of the initial analysis, using the same alignment, parameters and tree topology, resulted in times no more than 0.5% different from the initial analysis at each node. No single calibration had undue effects on the resulting times. Removal of individual minimum constraints resulted in times differing by less than two percent at any node. Removal of the single maximum constraint had slightly greater effects, resulting in times five percent older on average. Employing the complete sequence alignment (with chimeric sequences) also

TABLE 2. Times of divergence and Bayesian credibility intervals for nodes in Figure 11. The default analysis uses sequences of nine genes and the topology of the 17-gene ML analysis (Figure 8). Divergence times are also given for analyses after removal of individual calibrations, using sequence data from all 17 genes, and using the topology from the 9-gene ML analysis (Figure 10).

Node	Divergence Time	no 61 Ma cal.	no 35 Ma cal.	no 70 Ma cal.	no 16 Ma cal.
1	73.9 (99.7–53.0)	73.6 (100.0–52.2)	72.8 (99.4–49.7)	77.7 (115.9–53.5)	73.9 (100.0–53.2)
2	70.0 (94.5–50.2)	69.7 (94.3–49.5)	68.9 (94.2–46.9)	73.6 (110.4–50.4)	69.9 (94.5–50.5)
3	69.1 (93.2–49.6)	68.8 (93.2–48.9)	68.0 (93.0–46.2)	72.7 (108.8–49.8)	69.1 (93.2–49.9)
4	63.6 (86.6–45.3)	63.4 (86.8–44.4)	62.6 (86.3–42.0)	66.9 (101.1–45.5)	63.6 (86.8–45.6)
5	67.7 (91.4–48.6)	67.4 (91.3–47.8)	66.6 (91.2–45.3)	71.2 (106.8–48.8)	67.6 (91.4–48.8)
6	65.9 (89.1–47.1)	65.6 (89.1–46.4)	64.9 (89.1–44.0)	69.3 (104.0–47.4)	65.8 (89.0–47.4)
7	66.8 (90.2–47.9)	66.5 (90.0–47.2)	65.7 (90.1–44.6)	70.2 (105.8–48.1)	66.7 (90.2–48.2)
8	64.9 (87.7–46.5)	64.6 (87.7–45.7)	63.9 (87.5–43.2)	68.2 (102.7–46.6)	64.9 (87.6–46.8)
9	64.2 (86.9–45.9)	63.9 (86.6–45.2)	63.2 (86.7–42.8)	67.5 (101.7–46.2)	64.1 (86.9–46.1)
10	59.0 (80.6–41.4)	58.8 (81.1–40.7)	58.1 (80.9–38.8)	62.0 (94.3–41.8)	59.0 (80.8–41.7)
11	62.4 (84.5–44.6)	62.1 (84.4–43.9)	61.3 (84.3–41.6)	65.6 (98.8–44.8)	62.3 (84.2–44.8)
12	62.7 (84.6–44.9)	62.4 (84.5–44.4)	61.7 (84.6–41.6)	65.9 (99.2–45.2)	62.6 (84.3–45.1)
13	60.0 (81.4–42.8)	59.7 (81.5–42.1)	59.0 (81.2–40.0)	63.1 (95.2–43.0)	60.0 (81.4–42.9)
14	60.1 (81.7–42.9)	59.8 (81.6–42.2)	59.1 (81.4–40.0)	63.2 (95.8–43.0)	60.1 (81.7–43.1)
15	55.2 (75.4–38.8)	54.9 (75.4–38.3)	54.3 (75.6–36.5)	58.1 (88.1–39.1)	55.1 (75.7–39.1)
16	58.8 (79.9–42.0)	58.6 (79.8–41.3)	57.9 (79.7–39.1)	61.9 (93.7–42.0)	58.8 (79.8–41.9)
17	52.4 (72.2–36.7)	52.1 (72.2–36.3)	51.5 (71.7–34.3)	55.1 (84.1–37.0)	52.3 (71.7–36.8)
18	53.4 (73.4–37.5)	53.2 (73.3–36.9)	52.6 (73.4–35.2)	56.3 (85.4–37.8)	53.4 (73.3–37.7)
19	54.2 (73.9–38.4)	54.0 (73.7–37.9)	53.4 (73.8–36.0)	57.0 (86.2–38.7)	54.2 (73.9–38.8)
20	52.2 (71.2–36.9)	52.0 (71.1–36.4)	51.4 (71.1–34.6)	54.9 (83.0–37.2)	52.2 (71.1–37.2)
21	49.8 (68.2–35.1)	49.6 (67.9–34.6)	49.0 (68.0–32.9)	52.3 (79.4–35.4)	49.7 (68.2–35.4)
22	48.1 (65.9–33.8)	47.9 (65.9–33.5)	47.4 (65.7–31.4)	50.6 (77.1–34.3)	48.1 (66.1–34.0)
23	48.6 (66.8–34.3)	48.4 (66.4–33.7)	47.8 (66.5–32.0)	51.1 (77.8–34.6)	48.6 (66.6–34.5)
24	50.6 (67.9–36.2)	50.4 (67.9–36.0)	49.7 (68.0–33.1)	53.3 (81.5–36.4)	50.5 (67.9–36.4)
25	46.3 (65.1–31.5)	46.1 (65.3–30.9)	45.5 (65.0–29.6)	48.6 (75.4–31.6)	46.2 (65.4–31.4)
26	48.0 (65.8–33.8)	47.8 (65.4–33.2)	47.2 (65.5–31.5)	50.4 (76.7–34.1)	47.9 (65.8–34.0)
27	46.6 (64.2–32.4)	46.3 (63.9–32.0)	45.8 (64.2–30.5)	49.0 (74.7–32.7)	46.5 (64.1–32.7)
28	48.7 (67.1–34.0)	48.4 (67.3–33.4)	47.9 (66.7–31.9)	51.2 (78.2–34.3)	48.6 (66.9–34.3)
29	45.0 (62.0–31.3)	44.8 (62.1–30.8)	44.3 (61.8–29.6)	47.4 (72.4–31.9)	45.0 (62.2–31.6)
30	46.0 (63.4–32.2)	45.8 (63.3–31.7)	45.2 (63.5–29.9)	48.3 (73.8–32.3)	46.0 (63.2–32.3)
31	44.1 (60.8–30.7)	43.9 (605.–30.2)	43.3 (60.8–28.7)	46.3 (70.9–31.1)	44.0 (60.8–30.9)
32	39.9 (56.3–27.0)	39.6 (56.2–26.6)	39.2 (55.8–25.2)	41.9 (65.2–27.4)	39.8 (56.0–27.1)
33	41.5 (57.6–28.7)	41.3 (57.4–28.1)	40.8 (57.4–26.9)	43.6 (66.7–29.1)	41.4 (57.4–28.8)
34	35.5 (50.2–24.2)	35.3 (49.8–23.7)	34.9 (49.1–22.9)	37.3 (58.0–24.4)	35.4 (49.9–24.3)
35	34.5 (49.7–22.8)	34.3 (49.5–22.5)	33.9 (49.4–21.5)	36.2 (57.0–23.0)	34.4 (49.8–22.8)
36	31.8 (45.5–21.4)	31.7 (45.3–21.1)	31.3 (45.1–20.4)	33.5 (52.4–21.7)	31.8 (45.2–21.6)
37	31.3 (44.7–21.1)	31.2 (44.6–20.9)	30.8 (44.4–19.7)	32.9 (51.4–21.3)	31.3 (44.4–21.2)
38	34.1 (47.9–22.8)	33.9 (48.2–22.9)	33.6 (48.2–21.6)	35.9 (55.9–23.3)	34.1 (48.5–23.1)
39	22.2 (32.7–14.1)	22.0 (32.5–14.0)	21.7 (32.4–13.3)	23.4 (37.0–14.4)	22.1 (32.7–14.2)
40	1.2 (2.1–0.6)	1.2 (2.1–0.6)	1.2 (2.1–0.6)	1.3 (2.3–0.6)	1.2 (2.1–0.6)

continued.

Node	no 24 Ma cal.	no 15 Ma cal.	17-gene analysis	9-gene topology
1	73.9 (99.6–53.3)	73.8 (100.0–53.3)	77.4 (107.2–57.1)	73.0 (92.4–53.7)
2	69.9 (94.2–50.5)	69.9 (95.0–50.5)	71.3 (98.6–52.9)	x
3	69.1 (93.1–49.8)	69.0 (93.8–49.8)	69.1 (95.5–51.4)	x
4	63.6 (86.4–45.4)	63.6 (86.8–45.3)	67.5 (93.4–49.9)	61.7 (79.0–44.9)
5	67.6 (91.1–48.7)	67.6 (91.6–48.8)	67.2 (92.9–50.0)	x
6	65.8 (88.9–47.4)	65.8 (89.5–47.2)	66.1 (91.2–49.0)	65.6 (83.5–48.1)
7	66.7 (89.9–48.0)	66.7 (90.4–48.1)	65.6 (90.7–48.8)	x
8	64.9 (87.7–46.7)	64.8 (87.7–46.7)	64.7 (89.3–48.1)	71.9 (91.0–52.8)
9	64.1 (86.6–46.1)	64.1 (87.0–46.1)	63.8 (88.2–47.4)	68.0 (86.1–49.9)
10	59.0 (80.8–41.8)	59.0 (81.1–41.6)	62.5 (87.1–46.0)	57.0 (73.7–41.0)
11	62.3 (84.4–44.7)	62.3 (84.6–44.7)	62.3 (86.2–46.3)	66.1 (83.9–48.4)
12	62.6 (84.3–45.2)	62.6 (84.6–45.1)	61.3 (84.6–45.7)	68.0 (85.6–49.8)
13	60.0 (81.2–42.8)	59.9 (81.5–42.9)	60.9 (84.6–45.1)	63.7 (81.1–46.6)
14	60.0 (81.6–43.1)	60.0 (81.6–43.0)	58.9 (81.7–43.7)	66.7 (85.0–48.7)
15	55.1 (75.6–39.2)	55.1 (75.6–39.2)	57.0 (79.4–42.2)	60.8 (77.9–44.0)
16	58.8 (79.8–41.9)	58.7 (80.2–41.8)	56.7 (79.0–41.9)	62.5 (79.6–45.6)
17	52.3 (71.7–36.9)	52.3 (71.9–36.8)	56.1 (78.2–41.4)	55.6 (71.9–40.0)
18	53.4 (73.4–37.7)	53.4 (73.4–37.7)	53.9 (75.5–39.7)	59.0 (75.9–42.6)
19	54.2 (74.0–38.7)	54.2 (73.9–38.7)	52.5 (72.9–38.8)	60.4 (77.3–43.8)
20	52.2 (71.3–37.2)	52.2 (71.2–37.1)	51.1 (71.0–37.7)	57.9 (74.4–41.9)
21	49.7 (68.1–35.4)	49.8 (68.2–35.3)	48.5 (67.5–35.7)	54.9 (70.8–39.5)
22	48.1 (65.8–34.2)	48.1 (66.0–33.9)	47.6 (66.5–35.1)	53.0 (68.0–38.2)
23	48.6 (66.6–34.6)	48.6 (66.7–34.4)	47.4 (65.9–34.8)	53.8 (69.4–38.6)
24	50.6 (67.7–36.4)	50.5 (67.9–36.3)	47.1 (65.7–35.6)	55.9 (69.1–40.5)
25	46.2 (65.4–31.4)	46.2 (65.3–31.5)	47.0 (66.4–34.1)	48.8 (65.2–33.7)
26	47.9 (65.8–34.1)	47.9 (65.9–33.8)	46.6 (64.9–34.2)	x
27	46.6 (64.5–32.8)	46.6 (64.6–32.7)	46.1 (64.1–33.6)	45.7 (60.0–32.1)
28	48.6 (66.7–34.3)	48.6 (66.8–34.0)	45.9 (64.5–33.3)	51.7 (67.1–37.0)
29	45.0 (62.2–31.7)	45.0 (62.2–31.6)	44.7 (62.4–32.7)	x
30	46.0 (63.5–32.3)	45.9 (63.4–32.3)	44.2 (61.9–32.3)	51.3 (66.8–36.7)
31	44.0 (60.9–31.0)	44.1 (60.9–30.9)	44.0 (61.5–32.1)	49.8 (64.9–35.6)
32	39.8 (56.2–27.1)	39.8 (56.4–27.0)	41.7 (59.1–30.0)	42.2 (56.7–29.1)
33	41.4 (57.5–28.8)	41.4 (57.8–28.9)	41.3 (58.3–29.9)	45.7 (60.0–32.1)
34	35.4 (50.2–24.5)	35.4 (49.8–24.2)	36.1 (51.1–25.8)	37.5 (50.3–26.2)
35	34.4 (49.7–22.7)	34.4 (49.7–22.8)	33.5 (48.3–23.0)	33.7 (46.3–22.5)
36	31.8 (45.4–21.7)	31.8 (45.1–21.5)	33.1 (47.2–23.3)	33.8 (45.8–23.3)
37	31.3 (44.4–21.3)	31.3 (44.4–21.2)	31.2 (44.5–22.0)	35.0 (47.3–24.1)
38	34.1 (48.0–23.2)	34.1 (48.4–23.1)	31.2 (44.5–22.1)	37.9 (50.7–26.1)
39	22.2 (32.6–14.1)	22.1 (32.7–14.1)	21.1 (31.2–14.2)	23.6 (33.4–15.5)
40	1.2 (2.1–0.6)	1.2 (2.1–0.6)	1.1 (1.9–0.6)	1.4 (2.5–0.7)

had little effect, resulting in times differing by an average of one percent. Using the topology from the ML analysis of the reduced dataset had greater effects, resulting in times seven percent older on average. Recent molecular clock analyses of terraranans (Heinicke *et al.* 2007; Roelants *et al.* 2007) produced somewhat younger divergence times (ten percent on average) than this analysis, although results are more similar for some key nodes. The older dates obtained in this study may result from one of several potential causes, including differences in taxon sampling, phylogeny, and sequences used. These older inferred times do not affect previous hypotheses of terraranan biogeographic history (Heinicke *et al.* 2007; Hedges et al. 2008). The timetree indicates that *Craugastor* and *Haddadus* diverged in the early Cenozoic, about 42 (58–29) Ma, nearly identical to the previous estimate of 42 (59–31) Ma (Heinicke *et al.* 2007). *Eleutherodactylus* and *Diasporus* (not timed in Heinicke *et al.* 2007) diverged in the mid-Cenozoic, 32 (46–21) Ma. In contrast, previous studies based on immunological distances (Hedges *et al.* 1992; Hedges 1996) and DNA sequence data (Crawford & Smith 2005), and calibrated differently, obtained older time estimates indicating origins in the Late Cretaceous or early Cenozoic. The radiation leading to most other nobleobatrachian families occurred rapidly across the K-T boundary, similar to, but slightly older than, a previously-inferred explosive post-Cretaceous diversification (Roelants *et al.* 2007).

Outside Terrarana, even > 10 kb of sequence data are not able to resolve interfamilial relationships. Resolution of a major exception, the Terrarana + Hemiphractidae clade, is probably facilitated by the early-diverging position of Ceuthomantidae. This helps to break up the long phylogenetic branch leading to Terrarana, an action in general known to improve the accuracy of phylogenetic analysis (Heath *et al.* 2008). Most of the other basal branches in Nobleobatrachia are characterized by very short internodes (Fig. 8), which may confound efforts to resolve these early divergences even with increased gene sampling (Rokas & Carroll 2006; Wiens *et al.* 2008). Some recent analyses suggest that such short internodes are resolvable, however, and additional support may be provided through the discovery of shared rare genomic changes (e. g. Janečka *et al.* 2007). Resolution of these branches in future studies is critical to place into context the emergence of the most successful nobleobatrachian groups (bufonids, dendrobatoids, and hylids, in addition to terraranans) from the "leptodactylids" at the base of the tree.

Evolution of Direct Development in Noblebatrachia

Terrarana, including this new family of frogs, is part of an even larger radiation of frogs—Nobleobatrachia—distributed primarily in the New World and containing nearly half (3,224 species in 17 families) of all living amphibians (AmphibiaWeb 2009; Frost 2009). We propose here an unranked taxon within Noblebatrachia that includes Terrarana and Hemiphractidae based on their close phylogenetic relationship (Fig. 8) and sharing direct development among most species: Orthobatrachia (Greek: *ortho*, direct; and *batrachos*, frog). By linking together groups sharing the same, advanced, reproductive mode, the discovery of Ceuthomantidae and recognition of Orthobatrachia provides a better understanding of the evolution of direct development in anurans (Hanken et al. 1997; Callery et al. 2001), at least within the major group of direct-developing frogs in the Noblebatrachia.

Except for a single live-bearing (ovoviviparous) species, *Eleutherodactylus jasperi* Drewry and Jones (Wake, 1978), all terraranans presumably undergo direct development and lay large, terrestrial, unpigmented eggs that bypass the tadpole stage and hatch into froglets. Development has not been observed for most terraranan species, but direct development has been confirmed for at least some species in all families (excluding Ceuthomantidae), including one or more species in the genera *Brachycephalus*, *Ischnocnema*, *Craugastor*, *Eleutherodactylus*, *Diasporus*, *Barycholos*, *Bryophryne*, *Holoaden*, *Pristimantis*, *Psychrophrynella*, *Strabomantis* and *Yunganastes* (e. g. Pombal *et al.* 1994; Lynn & Lutz 1946; Valett & Jameson 1961; Schwartz & Henderson 1991; Ovaska & Rand 1991; Caramaschi & Pombal 2001; Catenazzi 2006; Lutz 1958; Hödl 1990; De la Riva 2007; Heatwole 1962; De la Riva & Lynch, 1997). Hemiphractids are unique in that the embryos of different species reflect various stages of development (Wassersug & Duellman 1984). Of the five genera of hemiphractids, all species in three (*Cryptobatrachus*, *Hemiphractus*, *Stefania*) have direct development; in *Flectonotus* eggs hatch as nonfeeding larvae with well-developed hind

limbs and forelimbs. Most species of *Gastrotheca* have direct development but in some others the eggs hatch at a range of developmental states (Duellman 2007). The Brazilian microhylid *Myersiella microps* Duméril and Bibron, along with several bufonids of the genera *Oreophrynella*, *Osornophryne* (presumed), and *Rhinella* (presumed) are the only non-orthobatrachians in the New World that have direct development of terrestrial eggs (Izecksohn *et al.* 1971; McDiarmid & Gorzula 1989; Gluesenkamp & Acosta 2001; Duellman & Trueb 1986).

Direct development also is characteristic *Arthroleptis* in Africa (Blackburn, 2008) and of two major clades in Southeast Asia and the Australo-Papuan Region (Ceratobatrachidae and asterophryine microhylids, respectively), as well as a few other frogs (Bossuyt & Milinkovitch 2000; Duellman 2007; Meegaskumbura *et al.* 2002; Pikacha *et al.* 2008). Together, the 975 species of orthobatrachian frogs with direct development include 73% of all direct-developing frog species in the World and 96% of those in the New World. A Bayesian molecular clock analysis shows the divergence between Terrarana and Hemiphractidae to be approximately 65 (48–89) Ma (Fig. 11, Table 2). This suggests that at least terrestrial reproduction, if not direct development, had evolved among South American frogs by that time.

Although terraranans and hemiphractids are both direct-developing groups, the degree of specialization and developmental attributes differ between them. The development of terraranans has been characterized as the most ontogenetically advanced of all frogs, such that most traces of the tadpole stage in the embryo have been lost (Thibaudeau & Altig 1999). Embryonic respiratory structures consist of an expanded, vascularized tail or small external gills derived from Branchial Arch III; these are reabsorbed prior to hatching (Duellman & Trueb 1986). In contrast, hemiphractid embryonic respiratory structures consist of large bell-shaped external gills derived from Branchial Arches I and II (Duellman & Trueb 1986). Direct-developing species of hemiphractids have retained enough larval characteristics such that the tadpole stage has been able to re-evolve one or more times in *Gastrotheca* and possibly *Flectonotus* (Duellman & Hillis 1987; Wassersug & Duellman 1984; Wiens *et al.* 2007). Unlike most aquatic frogs that have small, pigmented eggs, *Ceuthomantis cavernibardus* has large, unpigmented eggs typical of direct-developing species of terraranans. However, such eggs also are associated with frogs that have nonfeeding tadpoles, including hemiphractids (Duellman 2007; Wells 2007); therefore additional data are needed to confirm the reproductive mode of *Ceuthomantis*. Determination of the reproductive mode in Ceuthomantidae may provide insight into the origin of developmental differences between Terrarana and Hemiphractidae.

Discussion

The ancient highlands of the Guiana Shield represent a unique biogeographic region in South America where endemism is high, especially among certain groups of plants (Steyermark 1986), birds (Mayr & Phelps 1967), and amphibians (Señaris & MacCulloch 2005; McDiarmid & Donnelly 2005). Eight genera of anurans with 50 recognized species are endemic to the Guiana Highlands. In addition to *Ceuthomantis* with three species, there are two genera of bufonids—*Oreophrynella* (10 species) and the monotypic *Metaphryniscus*—two genera of hylids—*Myersiohyla* (4 species) and *Tepuihyla* (8 species)—the strabomantid genus *Dischidodactlyus* with two species (Ayarzagüena 1986; Lynch 1979); also there are the hemiphractid genus *Stefania* with 18 species (MacCulloch *et al.* 2006) and the monotypic dendrobatid genus *Minyobates*. In addition there are many endemic species including 15 *Pristimantis* (Strabomantidae) (e.g., Myers & Donnelly 2008), one clade of four species of *Hyalinobatrachium* and one species of *Vitreorana* (Centrolenidae) (Guayasamin *et al.* 2009), as well as eight species of *Anomaloglossus* (Dendrobatidae) and at least six species of *Hypsiboas* and one of *Osteocephalus* (Hylidae) (MacCulloch & Lathrop 2005). With exploration of many other tepuis or granitic mountains the number of endemic taxa certainly will increase significantly.

The discovery of *Ceuthomantis* highlights the importance of geologically old regions of continents, such as the Guiana Shield, for harboring relict biodiversity of evolutionary importance, as was emphasized in the discovery of Nasikabatrachidae in India (Biju & Bossuyt 2003; Hedges 2003). In addition to *Ceuthomantis*,

early-branching lineages of several frog families occur in this region, as shown by three other molecular phylogenies. The endemic treefrogs of the genus *Myersiella* are the closest relatives of the clade containing all of the other South American hylines (Faivovich *et al.*, 2005). *Minyobates* seems to be the closest relative of all other dendrobatine frogs (Grant *et al.* 2006). The hemiphractid genus *Stefania* is basal to the genus *Gastrotheca* (Wiens *et al.* 2007). Whereas geologically active areas, such as the Andes, may have higher rates of speciation, the older, more stable regions may act as evolutionary refugia for "living fossils." These early-branching lineages can provide a wealth of biological information far beyond that which can be gleaned from fossils alone.

Acknowledgments

References

Alberch, P. & Gale, E.A. (1985) A developmental analysis of an evolutionary trend: digital reduction in amphibians. *Evolution*, 39, 8–23.

AmphibiaWeb. (2009) AmphibiaWeb: information on amphibian biology and conservation (http://amphibiaweb.org/), accessed: 14 June 2009. University of California, Berkeley, California

Ayarzagüena, J. (1985 "1983") Una nueva especie de *Dischidodactylus* Lynch (Amphibia, Leptodactylidae) en la cumbre del Tepui Marahuaca, Territorio Federal Amazonas – Venezuela. *Memorias Sociedad de Ciencias Naturales La Salle,* 43, 215–220.

Báez, A.M. (2000) Tertiary anurans from South America. *In:* Heatwole, H. & Carrol, R.L. (Eds.) *Amphibian biology, Volume 4: Paleontology.* Surrey Beatty & Sons, Chipping Norton, Australia, pp. 1388–1401.

Báez, A.M. & Nicoli, L. (2004) Bufonid toads from the late Oligocene beds of Salla, Bolivia. *Journal of Vertebrate Paleontology*, 24, 73–79.

Barrio-Amorós, C.L. & Brewer-Cariás, C. (2008) Herpetological results of the 2002 expedition to Sarisariñama, a tepui in Venezuela Guayana, with the description of five new species. *Zootaxa,* 1942, 3–68.

Barrio-Amorós, C.L. & Molina, C.R. (2006) A new *Eleutherodactylus* (Anura, Brachycephalidae) from the Venezuelan Guayana, and redescription of *Eleutherodactylus vilarsi* (Melin). *Zootaxa*, 1302, 1–20.

Biju, S.D. & Bossuyt, F. (2003) New frog family from India reveals an ancient biogeographical link with the Seychelles. *Nature*, 425, 711–714.

Blackburn, D.C. (2008) Biogeography and evolution of body size and life history of African frogs: phylogeny of squeakers (*Arthroleptis*) and long-fingered frogs (*Cardioglossa*) estimated from mitochondrial data. *Molecular Phylogenetics and Evolution,* 49, 802–826.

Bossuyt, F. & Milinkovitch, M.C. (2000) Convergent adaptive radiations in Madagascan and Asian ranid frogs reveal covariation between larval and adult traits. *Proceedings of the National Academy of Sciences of the United States of America*, 97, 6585–6590.

Callery, E.M., Fang, H., & Elinson, R.P. (2001) Frogs without polliwogs: evolution of anuran direct development. *Bioessays*, 23, 233–241.

Caramaschi, U. & Pombal, J.P., Jr. (2001) *Barycholos savagei*: a junior synonym of *Paludicola ternetzi*, with notes on development. *Journal of Herpetology*, 35, 357–360.

Castresana, J. (2000) Selection of conserved blocks from multiple alignments for their use in phylogenetic analysis. *Molecular Biology and Evolution*, 17, 540–552.

Catenazzi, A. (2006) *Phrynopus cophites*. Reproduction. *Herpetological Review*, 37, 206.

Crawford, A.J. & Smith, E.N. (2005) Cenozoic biogeography and evolution in direct-developing frogs of Central America (Leptodactylidae: *Eleutherodactylus*) as inferred from a phylogenetic analysis of nuclear and mitochondrial genes. *Molecular Phylogenetics and Evolution*, 35, 536–555.

Darst, C.R. & Cannatella, D.C. (2004) Novel relationships among hyloid frogs inferred from 12S and 16S mitochondrial DNA sequences. *Molecular Phylogenetics and Evolution*, 31, 462–475.

De la Riva, I. (2007) Bolivian frogs of the genus *Phrynopus*, with the description of twelve new species (Anura: Brachycephalidae). *Herpetological Monographs*, 21, 241–277.

De la Riva, I. & Lynch, J.D. (1997) New species of *Eleutherodactylus* from Boliva (Amphibia: Leptodactylidae). *Copeia*, 1997, 151–157.

Doyle, A.C. (1912) *The Lost World.* Hodder & Stoughten, London, 192 pp.

Dubois, A. (2009) Miscellanea nomenclatorica batrachologica 20. Class-series nomina are nouns in the nominative plural. *Alytes,* 26, 167–175.

Duellman, W.E. (2007) Amphibian life histories: their utilization in phylogeny and classification. *In:* Heatwole, H. & Tyler, M. (Eds.) *Amphibian Biology, Vol. 7 Systematics.* Surrey Beatty & Sons, Chipping Norton, NSW, Australia, pp. 2843–2892.

Duellman, W.E. & Hillis, D.M. (1987) Marsupial frogs (Anura, Hylidae, *Gastrotheca*) of the Ecuadorian Andes: resolution of taxonomic problems and phylogenetic relationships. *Herpetologica*, 43, 141–173.

Duellman, W.E. & Pramuk, J.B. (1999) Frogs of the genus *Eleutherodactylus* (Anura: Leptodactylidae) in the Andes of northern Peru. *Scientific Papers Natural History Museum University of Kansas,* 13, 1–78.

Duellman, W.E. & Trueb, L. (1986) *Biology of Amphibians*. McGraw-Hill, New York, 670 pp.

Edgar, R.C. (2004) MUSCLE: multiple sequence alignment with high accuracy and high throughput. *Nucleic Acids Research*, 32, 1792–1797.

Fabrezi, M. & Alberch, P. (1996) The carpal elements of anurans. *Herpetologica*, 52, 188–204.

Faivovich, J., Haddad, C.F.B., Garcia, P.C.A., Frost, D.R., Campbell, J.A. & Wheeler, W.C. (2005) Systematic review of the frog family Hylidae, with special reference to Hylinae: phylogenetic analysis and taxonomic revision. *Bulletin of the American Museum of Natural History*, 294, 1–228.

Frost, D.R., Grant, T., Faivovich, J., Bain, R.H., Haas, A., Haddad, C.F.B., De Sa, R.O., Channing, A., Wilkinson, M., Donnellan, S.C., Raxworthy, C.J., Campbell, J.A., Blotto, B.L., Moler, P., Drewes, R.C., Nussbaum, R.A., Lynch, J.D., Green, D.M. & Wheeler, W.C. (2006) The amphibian tree of life. *Bulletin of the American Museum of Natural History*, 297, 1–371.

Frost, D.R. (2009) Amphibian species of the World: an online reference. Version 5.3 (http://research.amnh.org/herpetology/amphibia/index.php/), accessed 14 May 2009. American Museum of Natural History, New York.

Gluesenkamp, A.G. & Acosta, N. (2001) Sexual dimorphism in *Osornophryne guacamayo* with notes on natural history and reproduction in the species. *Journal of Herpetology*, 35, 148–151.

Grant, T., Frost, D.R., Caldwell, J.P., Gagliardo, R., Haddad, C.F.B., Kok, P.J.R., Means, D.B., Noonan, B.P., Schargel, W.E. & Wheeler, W.C. (2006) Phylogenetic systematics of dart-poison frogs and their relatives (Amphibia: Athesphatanura: Dendrobatidae). *Bulletin of the American Museum of Natural History*, 299, 1–262.

Guayasamin, J.M., Castroviejo-Fisher, S., Ayarzagüena, J., Trueb, L., & Vilà, C. (2008) Phylogenetics of glassfrogs (Centrolenidae) based on mitochondrial and nuclear genes. *Molecular Phylogenetics and Evolution,* 48, 574–595.

Guayasamin, J.M., Castroviejo-Fisher, S., Trueb, L., Ayarzagüena, J., Rada, M., & Vilà, C. (2009) Phylogenetic systematics of glassfrogs (Amphibia: Centrolenidae) and their sister taxon *Allophryne ruthveni. Zootaxa,* 2002, 1–97.

Hanken J., Jennings, D.H., & Olsson, L. (1997) Mechanistic basis of life-history evolution in anuran amphibians: direct development. *American Zoologist,* 37, 160–171.

Heath, T.A., Hedtke, S.M. & Hillis, D.M. (2008) Taxon sampling and the accuracy of phylogenetic analyses. *Journal of Systematics and Evolution*, 46, 239–257.

Heatwole, H. (1962) Contributions to the natural history of *Eleutherodactylus cornutus maussi. Stahlia*, 2, 1–7.

Hedges, S.B. (1989) Evolution and biogeography of West Indian frogs of the genus *Eleutherodactylus*: slow-evolving loci and the major groups. *In* C.A. Woods (Ed.), *Biogeography of the West Indies: past present and future*. Sandhill Crane Press, Gainesville, Florida, pp. 305–370.

Hedges, S.B. (1996) The origin of West Indian amphibians and reptiles. *In* Powell, R. & Henderson, R.W. (Eds.), *Contributions to West Indian herpetology: a tribute to Albert Schwartz.* Society for the Study of Amphibians and

Reptiles, Ithaca, New York, pp. 95-128.

Hedges, S. B. (2003) The coelacanth of frogs. *Nature,* 425, 669–670.

Hedges, S.B., Duellman, W.E., & Heinicke, M.P. (2008) New World direct-developing frogs (Anura: Terrarana): Molecular phylogeny, classification, biogeography, and conservation. *Zootaxa*, 1737, 1–182.

Hedges, S.B., Hass, C.A., & Maxson, L.R. (1992) Caribbean biogeography: molecular evidence for dispersal in West Indian terrestrial vertebrates. *Proceedings of the National Academy of Sciences (USA)*, 89, 1909–1913.

Heinicke, M.P., Duellman, W.E. & Hedges, S.B. (2007) Major Caribbean and Central American frog faunas originated by oceanic dispersal. *Proceedings of the National Academy of Sciences (USA)*, 104, 10092–10097.

Hödl, W. (1990) Reproductive diversity in Amazonian lowland frogs. *Fortschritte der Zoologie*, 38, 41–60.

Huber, O., Gharbarran, G., & Funk, V. (1995) Vegetation map of Guyana. Center for the Study of Biological Diversity, University of Guyana, Georgetown, Guyana.

Huelsenbeck, J.P., and Ronquist, F. (2001) Mr. Bayes: Bayesian inference of phylogenetic tree. *Bioinformatics Applications Note,* **17,** 754–755.

Iturralde-Vinent, M.A. & MacPhee, R.D.E. (1996) Age and paleogeographical origin of Dominican amber. *Science*, 273, 1850–1852.

Izecksohn, E., Jim, J., De Albuquerque, T.S., & De Mendonça, W.F. (1971) Observaçãos sôbre o desenvolvimento e os hábitos de *Myersiella subnigra* (Miranda-Ribeiro). *Arquivos do Museu Nacional Rio de Janeiro,* 54, 69–73.

Janečka, J.E., Miller, W., Pringle, T.H., Wiens, F., Zitzmann, A., Helgen, K.M., Springer, M.S., Murphy, W.J. (2007) Molecular and genomic data identify the closest living relative of primates. *Science*, 318, 792–794.

Li, Z.X. & Powell, C.M. (2001) An outline of the palaeogeographic evolution of the Australasian region since the beginning of the Neoproterozoic. *Earth-Science Reviews*, 53, 237–277.

Lutz, B. (1958) Anfíbios novos e raros das Serras Costeiras do Brasil. *Memórias do Instituto Oswaldo Cruz*, 56, 373–405.

Lynch, J.D. (1971) Evolutionary relationships, osteology, and zoogeography of leptodactyloid frogs. *Miscellaneous Publications of the University of Kansas, Museum of Natural History,* 53, 1–238.

Lynch, J.D. (1973) The transition from archaic to advanced frogs. *In* J.L. Vial (Ed.), *Evolutionary biology of the anurans: contemporary research on major problems*. University of Missouri Press, Columbia, pp. 133–182.

Lynch, J.D. (1979) A new genus for *Elosia duidensis* Rivero (Amphibia, Leptodactylidae) from southern Venezuela. *American Museum Novitates,* 2680, 1–8.

Lynch, J.D. (1986) The definition of the Middle American clade of *Eleutherodactylus* based in jaw musculature (Amphibia: Leptodactylidae). *Herpetologica,* 42, 248–258.

Lynch, J.D. & Duellman, W.E. (1997) Frogs of the genus *Eleutherodactylus* in western Ecuador. *University of Kansas Special Publication*, 23, 1–236.

Lynn, W.G. & Lutz, B. (1946) The development of *Eleutherodactylus guentheri* Stdnr. 1864. *Boletim do Museu Nacional Rio de Janeiro, Nova Serie, Zoologia*, 71, 1–46.

MacCulloch, R.D. & Lathrop, A. (2005) Hylid frogs from Mount Ayanganna, Guyana: new species, redescriptions, and distributional records. *Phyllomedusa,* 4, 17–37.

MacCulloch, R.D., Lathrop, A., & Khan, S.Z. (2006) Exceptional diversity of *Stefania* (Cryptobatrachidae) II: Six species from Mount Wokomung, Guyana. *Phyllomedusa,* 5, 31–41.

Mayr, E. & Phelps, Jr., W.H. (1967) The origin of the bird fauna of the south Venezuelan highlands. *Bulletin of the American Museum of Natural History*, 136, 269–328.

McDiarmid, R.W. & Donnelly, M.A. (2005) The herpetofauna of the Guayana Highlands: amphibians and reptiles of the Lost World. *In:* Donnelly, M.A., Crother, B.I., Guyer, C., Wake, M.H. & White, M.E. (Eds.) *Ecology and evolution in the tropics; a herpetological perspective*. University of Chicago Press, Chicago, pp. 461–560.

McDiarmid, R.W. & Gorzula, S. (1989) Aspects of the reproductive ecology and behavior of the tepui toads, genus *Oreophrynella* (Anura: Bufonidae). *Copeia*, 1989, 445–451.

Meegaskumbura, M., Bossuyt, F., Pethiyagoda, R., Manamendra-Arachchi, K., Bahir, M., Milinkovitch, M.C. & Schneider, C.J. (2002) Sri Lanka: An amphibian hot spot. *Science*, 298, 379–379.

Myers, C.W. & Donnelly, M.A. (1997) A tepui herpetofauna on a granitic mountain (Tamacuari) in the borderland between Venezuela and Brazil: report from the Phipps Tapirapecó Expedition. *American Museum Novitates*, 3213, 1–71.

Myers, C.W. & Donnelly, M.A. (2008) The summit herpetofauna of Auyantepui, Venezuela: report from the Robert G. Goelet American Museum-Terramar Expedition. *Bulletin of the American Museum of Natural History,* 308, 1–147.

Ovaska, K. & Rand, A.S. (2001) Courtship and reproductive behavior of the frog *Eleutherodactylus diastema* (Anura: Leptodactylidae) in Gamboa, Panama. *Journal of Herpetology*, 35, 44–50.

Pikacha, P., Morrison, C. & Richards, S. (2008) *Frogs of the Solomon Islands*. Institute of Applied Sciences, University of the South Pacific, Suva, Fiji, 68 pp.

Poinar, G.O. & Cannatella, D.C. (1987) An Upper Eocene frog from the Dominican Republic and its implication for Caribbean biogeography. *Science*, 237, 1215–1216.

Pombal, J.P., Jr., Sazima, I. & Haddad, C.F.B. (1994) Breeding behavior of the pumpkin toadlet, *Brachycephalus ephippium* (Brachycephalidae). *Journal of Herpetology*, 28, 516–519.

Posada, D. & Crandall, K.A. (1998) Modeltest: testing the model of DNA substitution. *Bioinformatics*, 14, 817–818.

Rambaut, A. & Drummond, A. (2005) Tracer version 1.3. (http://tree.bio.ed.ac.uk/software/tracer/). University of Oxford, Oxford

Roelants, K. & Bossuyt, F. (2005) Archaeobatrachian paraphyly and Pangaean diversification of crown-group frogs. *Systematic Biology*, 54, 111–26.

Roelants, K., Gower, D.J., Wilkinson, M., Loader, S.P., Biju, S.D., Guillaume, K., Moriau, L. & Bossuyt, F. (2007) Global patterns of diversification in the history of modern amphibians. *Proceedings of the National Academy of Sciences of the United States of America*, 104, 887–892.

Rokas, A., Carroll, S.B. (2006) Bushes in the tree of life. *PLOS Biology*, 4, e352.

Sanchiz, F.B. (1998) Vertebrates from the Early Miocene lignite deposits of the opencast mine Oberdorf (western Styrian Basin, Austria). 2. Amphibia. *Annalen des Naturhistorischen Museums in Wien*, 99, 13–29.

Sanmartin, I. & Ronquist, F. (2004) Southern Hemisphere biogeography inferred by event-based models: Plant versus animal patterns. *Systematic Biology*, 53, 216–243.

Schwartz, A. & Henderson, R.W. (1991) *Amphibians and Reptiles of the West Indies: Descriptions, Distributions, and Natural History*. University Press of Florida, Gainesville, 720 pp.

Señaris, J.D. & MacCulloch, R. (2005) Amphibians. *In:* Hollowell, T. & Reynolds, R (Eds.) *Checklist of the terrestrial vertebrates of the Guiana Shield. Bulletin of the Biological Society of Washington,* 13, 8–23.

Shubin, N. & Alberch, P. (1986) A morphogenetic approach on the origin and basic organization of the tetrapod limb. *In:* Hecht, M., Wallace, B. & Prance, G. (Eds.) *Evolutionary Biology*. Plenum Press, New York, USA, pp. 319–387.

Springer, M.S., Westerman, M., Kavanagh, J.R., Burk, A., Woodburne, M.O., Kao, D.J. & Krajewski, C. (1998) The origin of the Australasian marsupial fauna and the phylogenetic affinities of the enigmatic monito del monte and marsupial mole. *Proceedings of the Royal Society of London Series B-Biological Sciences*, 265, 2381–2386.

Stamatakis, A. (2006) RAxML-VI-HPC: maximum likelihood-based phylogenetic analyses with thousands of taxa and mixed models. *Bioinformatics*, 22, 2688–2690.

Steyermark, J.A. (1986) Speciation and endemism in the flora of the Venezuelan tepuis. *In:* Vuilleumier, F. & Monasterío, M. (Eds.) *High Altitude Tropical Biogeography,* Oxford University Press, New York, USA, pp. 317–373.

Stocsits, R.R. (2009) *RNAsalsa. Web resource available at: http://www.zfmk.de/web/Forschung/Abteilungen/AG_Wgele/Software/index.en.html*. Museumsmeile Bonn, Bonn, Germany.

Tamura, K., Dudley, J., Nei, M., Kumar, S. (2007) MEGA4: Molecular evolutionary genetics analysis (MEGA) software version 4.0. *Molecular Biology and Evolution*, 24, 1596–1599.

Thibaudeau, G. & Altig, R. (1999) Endotrophic Anurans: Development and Evolution. *In:* McDiarmid, R.W. & Altig, R. (Eds.) *Tadpoles: The Biology of Anuran Larvae*. University of Chicago Press, Chicago, USA, pp. 170–188.

Thorne, J.L. & Kishino, H. (2002) Divergence time and evolutionary rate estimation with multilocus data. *Systematic Biology*, 51, 689–702.

Trueb, L. (1977) Osteology and anuran systematics: Intrapopulational variation in *Hyla lanciformis. Sysytematic Zoology*, 26, 165–184.

Trueb, L. (1993) Patterns of cranial diversity among the Lissamphibia. *In:* J. Hanken, J. & Hall, B.K. *The skull. Volume 2. Patterns of structural and systematic diversity.* University of Chicago Press, Chicago. pp. 255–343.

Valett, B.B. & Jameson, D.L. (1961) The embryology of *Eleutherodactylus augusti latrans*. *Copeia*, 1961, 103–109.

Wake, M.H. (1978) The reproductive biology of *Eleutherodactylus jasperi* (Amphibia, Anura, Leptodactylidae), with comments on the evolution of live-bearing systems. *Journal of Herpetology,* 12, 121–133.

Wassersug, R.J. & Duellman, W.E. (1984) Oral structures and their development in egg-brooding hylid frog embryos and larvae: evolutionary and ecological implications. *Journal of Morphology*, 182, 1–37.

Wells, K.D. (2007) *The ecology and behavior of amphibians*. University of Chicago Press, Chicago, 1148 pp.

Wiens, J.J., Fetzner, J.W., Parkinson, C.L. & Reeder, T.W. (2005) Hylid frog phylogeny and sampling strategies for speciose clades. *Systematic Biology*, 54, 719–748.

Wiens, J.J., Kuczynski, C.A., Duellman, W.E. & Reeder, T.W. (2007) Loss and re-evolution of complex life cycles in marsupial frogs: Does ancestral trait reconstruction mislead? *Evolution*, 61, 1886–1899.

Wiens, J.J., Kuczynski, C.A., Smith, S.A., Mulchay, D.G., Sites, J.W., Jr., Townsend, T.M. & Reeder, T.W. (2008) Branch lengths, support, and congruence: testing the phylogenomic approach with 20 nuclear loci in snakes. *Systematic Biology*, 57, 420–431.

Woodburne, M.O. & Case, J.A. (1996) Dispersal, vicariance, and the late Cretaceous to early Tertiary land mammal biogeography from South America to Australia. *Journal of Mammalian Evolution*, 3, 121–161.

Xia, X. & Xie, Z. (2001) DAMBE: Software package for data analysis in molecular biology and evolution. *Journal of Heredity*, 92, 371–373.

Yang, Z. & Yoder, A.D. (2003) Comparison of likelihood and Bayesian methods for estimating divergence times using

multiple gene Loci and calibration points, with application to a radiation of cute-looking mouse lemur species. *Systematic Biology*, 52, 705–716.

Appendix 1. Specimens newly sequenced for molecular analyses.

Species	Lab tissue number	Museum voucher	Locality
Rhinella margaritifera	268430	MSH 5249-50	French Guiana: Petit-Saut, Sinnamary River
Phyllomedusa hypochondrialis	268431	USNM-FS 46785	Brazil: Rio Tapajos
Flectonotus fitzgeraldi	268432	KU 192399–400	Trinidad and Tobago: Trinidad, 6.4 km N Arima
Stefania ginesi	268433	LM 1056	Venezuela: Amazonas, Abacapa Tepui
Hemiphractus bubalus	268434	KU 178588	Ecuador: Pastaza, Mera
Mannophryne trinitatus	171009	n/a	Trinidad and Tobago: Trinidad, Paria River (near Brasso Seco)
Mannophryne trinitatus	268435	UIMNH 94439–441	Trinidad and Tobago: Trinidad, Arima-Blanchisseuse Road
Brachycephalus ephippium	268117	USNM 207716	Brazil: São Paulo, Eugenio Lefevre
Ischnocnema guentheri	267345	USNM-FS 053312	Brazil: São Paulo, Estação Biológica de Jureia
Ischnocnema parva	267328	USNM-FS 053232	Brazil: São Paulo, Estação Biológica de Boracéia
Craugastor fitzingeri	194926	FMNH 257745	Costa Rica: Puntarenas, Wilson Botanical Garden
Craugastor podiciferus	266082	MVZ 12020	Costa Rica: Heredia, Chompipe, vicinity of Volcán Barba
Haddadus binotatus	267339	USNM 303077	Brazil: São Paulo, Estação Biológica de Boracéia
Eleutherodactylus cooki	160048	USNM 326784	USA: Puerto Rico, El Yunque
Eleutherodactylus planirostris	267470	n/a	USA: Florida, Monroe Co., Key West
Diasporus diastema	268025	MVZ 203844	Costa Rica: Cartago, 1.9 km S Tapanti Bridge over Río Grande de Orosi
Adelophryne gutturosa	268015	ROM 39578	Guyana: District 7, Mount Ayanganna
Pristimantis cruentus	267876	AMNH 12444–448	Panama: Ratibor, Finca Ojo de Agua
Phrynopus bracki	171045	USNM 286919	Peru: Pasco, 2.9 km N, 5.5 km E Oxapampa
Hypodactylus brunneus	267860	KU 178258	Ecuador: Carchí, 14.6 km NW Carchí
Hypodactylus dolops	267862	JDL 17574	Colombia
Strabomantis biporcatus	268087	CVULA 7073	Venezuela: Sucre, Parque Nacional de Pária, Las Melenas, Peninsula de Pária
Strabomantis necerus	267885	KU 179076	Ecuador: Carchí, Maldonado
Psychrophrynella wettsteini	268101	KU 183049	Bolivia: La Paz, 2.3 km S Unduavi
Psychrophrynella usurpator	267889	KU 173495	Peru: Cusco, Abra Acanacu, 25 km NNE Paucartambo
Ceuthomantis smaragdinus	268011	ROM 40161	Guyana: District 7, Mount Ayanganna
Ceuthomantis smaragdinus	268267	KU 315000	Guyana: Potaro-Siparuni, Wokomung Massif, Mt. Kopinang
Ceuthomantis smaragdinus	268268	KU 300000	Guyana: Potaro-Siparuni, Wokomung Massif, Mt. Kopinang
Proceratophrys melanopogon	268436	USNM 208125	Brazil: São Paulo; São José de Barreiro, Fazada de Vendo

Thoropa taophora	268437	USNM 209318	Brazil: Salesopolis, near Estação Biológica de Boracéia
Hylodes nasus	268438	USNM 245925	Brazil: Rio de Janiero, near Parque Nacional de Tijuca
Pleurodema marmoratum	268439	KU 173341	Peru: Cuzco, 36 km NW Ollantaytambo, Abra Málaga
Limnodynastes tasmaniensis	268440	n/a	Australia: Tasmania, Hamilton, Greenwich House

Appendix 2. Genbank accession numbers. Numbers with "GQ" are new to this study. Aligned sequence length is given for each gene. For ND1 and CytB, length after removal of third codon positions is given in parentheses.

Taxon	12S/tRNAV/16S	tRNAL/ND1	CytB	28S	c-myc A
Melanophryniscus	AY325999	AY819463 AY948744	DQ502444	AY844306	AY819167
Rhinella	AY843573 AY819331/AF375514	AY819461	AY843795	AY844205	AY819165
Duttaphrynus	AY458592	AY458592	AY458592	DQ283658	
Espadarana/Nymphargus	AY843574	AY819466	AY843796	AY844206	AY819170
Allophryne	AY843564	AY819458	AY843786		AY819162
Trachycephalus	AY326048	AY819514	EU034077	AY844322	AY819217
Hyla	EF566960	AY819494	AY843824	AY844241	AY819197
Acris	EF566970	AY819491	AY843782	AY844194	AY819194
Litoria	AY326038	AY819531	AY843938	AY844304	AY819234
Phyllomedusa	AY843724	AY819535 AY948748	AY843969	AY844329	AY819239
Flectonotus	AY843589 AY819355/DQ679381	AY819486	AY843809	AY844215	AY819189
Stefania	AY843768 DQ679266/DQ679417	AY819490 DQ679373	AY844013	AY844354	AY819193
Hemiphractus	AY843594 DQ679263/DQ679412	AY819489 DQ679370	AY843813	GQ345134	AY819192
Mannophryne/Allobates	DQ502131	AY819469	DQ502562	DQ503024	AY819173
Dendrobates/Hyloxalus	AY364565	AY819470	DQ502491	AY844211	AY819174
Epipedobates	AY364577		DQ502584	DQ283461	
Brachycephalus	AY326008	GQ345243	GQ345195	DQ282494	GQ345145
Ischnocnema	EF493533	GQ345244	GQ345196	DQ283495	EU025679
Craugastor	EF493360	GQ345245	GQ345197	DQ283648	GQ345146
Haddadus	EF493361		GQ345198	DQ283493	GQ345147
Eleutherodactylus	EF493539 GQ345176	GQ345246	GQ345199	DQ283629	AY211282
Diasporus	EU186682		GQ345200	GQ345135	GQ345148
Adelophryne	EU186679	GQ345247	GQ345201	GQ345136	GQ345149
Pristimantis	EF493697	AY948758	EU368884	AY844213	AY819177
Phrynopus	EF493709		GQ345202	GQ345137	GQ345150

Hypodactylus	EF493357	GQ345248	GQ345203	GQ345138	GQ345151
Strabomantis	EU186691	GQ345249	GQ345204	DQ283555	GQ345152
Psychrophrynella	EU186696	GQ345250	GQ345205	GQ345139	GQ345153
Ceuthomantis-W1	GQ345132	GQ345251	GQ345206	GQ345140	GQ345154
Ceuthomantis-W2	GQ345133	GQ345252	GQ345207	GQ345141	GQ345155
Ceuthomantis-A	EU186677	GQ345253	GQ345208	GQ345142	GQ345156
Batrachyla	AY843572 AY389157	AY948759	AY843794	AY844204	
Ceratophrys	AY326013	AY523774	AY843797	AY844207	AY819176
Lepidobatrachus	DQ283152	AY819475		DQ283543	AY819179
Telmatobius	DQ283040 DQ347049/DQ347333	AY819478	DQ502448	AY844355	AY819182
Odontophrynus/Proceratophrys	AY843704	AY948757	AY843949	AY844309	GQ345157
Thoropa	DQ283331	GQ345254	DQ502607	GQ345143	GQ345158
Rhinoderma/Cycloramphus	DQ283324	AY523783	DQ502589	DQ283654	
Hylodes	DQ502171	GQ345255	DQ502606	DQ503009	GQ345159
Pleurodema	AY843733	AY948753	AY843979	GQ345144	GQ345160
Physalaemus/Engystomops	AY843729 DQ337249	AY819477	AY843795	AY844330	AY819181
Leptodactylus	AY843688 AY364359/DQ347060	AY948760	AY843934	AY844302	AY337266
Calyptocephalella	DQ283439	AY819471		DQ283748	AY819175
Myobatrachidae	DQ283221	AY948768	AY843988	DQ283644	AY819185
Limnodynastidae	AY326071	AY523775	GQ345209	DQ283643	GQ345161
Ranidae	AY326063	M57527 AF314018	AY522428	DQ283522	AY819188
Sequence Length (bp)	835 / 73 / 1399	73 / 813 (542)	385 (256)	662	420

continued.

Taxon	c-myc B	CXCR4	HH3	NCX1	POMC	RAG-1 A
Melanophryniscus	AY819247	AY948784	DQ284060	AY948822	AY819082 DQ158263	AY948927
Rhinella	AY819244	DQ306529	DQ284103	GQ345223	AY819080	DQ158354
Duttaphrynus		AY364167	DQ284324	AY948805	DQ158317	AY364197
Espadarana/Nymphargus	AY819250	AY364193	DQ284066	AY948834	AY819085	AY364223
Allophryne	AY819242				AY819077	
Trachycephalus	AY819291	AY364185	DQ284097	AY948824	AY819132	AY364215
Hyla	AY819271	AY364190	DQ284057	EF107241	AY819112	AY364220
Acris	AY819268	EF107468	DQ284107	EF107244	AY819109	EF107304
Litoria	AY819308	AY948783	DQ284098	AY948821	AY819149	AY948926
Phyllomedusa	AY819313	AY948786	GQ345210	AY948826	AY819153	AY948929
Flectonotus	AY819265	GQ345177		GQ345224	AY819104	DQ679274

Stefania	AY819267	GQ345178	GQ345211	GQ345225	AY819108 DQ679338	DQ679308
Hemiphractus	AY819266	GQ345179	DQ284084	GQ345226	DQ679335	DQ679303
Mannophryne/Allobates	AY819253		DQ502347	GQ345227	AY819088	GQ345274
Dendrobates/Hyloxalus	AY819254	AY364184	DQ284072	AY948823	AY819089	AY364214
Epipedobates		EF107458	DQ502355	EF107233		EF107295
Brachycephalus	GQ345162	GQ345180	GQ345212	GQ345228	GQ345256	GQ345275
Ischnocnema	GQ345163	GQ345181	DQ284143	GQ345229	GQ345257	GQ345276
Craugastor	GQ345164	GQ345182	DQ284317	GQ345230	GQ345258	GQ345277
Haddadus	GQ345165	GQ345183	DQ284142	GQ345231	GQ345259	GQ345278
Eleutherodactylus	GQ345166	EF107500	GQ345213	EF107282	GQ345260	EF107341
Diasporus		GQ345184	GQ345214	GQ345232	GQ345261	GQ345279
Adelophryne	GQ345167	GQ345185	GQ345215	GQ345233	GQ345262	GQ345280
Pristimantis	AY819256	AY948792	GQ345216	AY948836	DQ158260	AY948935
Phrynopus	GQ345168	GQ345186	GQ345217	GQ345234	GQ345263	GQ345281
Hypodactylus		GQ345187	GQ345218	GQ345235	GQ345264	GQ345282
Strabomantis		GQ345188	DQ284203	GQ345236	GQ345265	GQ345283
Psychrophrynella		GQ345189	GQ345219	GQ345237	GQ345266	GQ345284
Ceuthomantis-W1	GQ345169	GQ345190	GQ345220	GQ345238	GQ345267	GQ345285
Ceuthomantis-W2		GQ345191	GQ345221	GQ345239	GQ345268	GQ345286
Ceuthomantis-A	GQ345170	GQ345192	GQ345222	GQ345240	GQ345269	GQ345287
Batrachyla		AY948793	DQ284119	AY948837		AY948936
Ceratophrys	AY819255	AY364188		AY523718	AY819091	AY364218
Lepidobatrachus	AY819258	EF107461	DQ284191	EF107236	AY819094	EF107298
Telmatobius	AY819260	EF107464	DQ284068	EF107239	AY819097	DQ347275
Odontophrynus/ Proceratophrys	GQ345171	AY948791	DQ284273	AY948835	GQ345270	AY948934
Thoropa	GQ345172	GQ345193	DQ502369	GQ345241	GQ345271	GQ345288
Rhinoderma/Cycloramphus		AY364192	DQ284320	AY523733		AY364222
Hylodes	GQ345173	GQ345194	DQ502368	GQ345242	GQ345272	GQ345289
Pleurodema	GQ345174	AY948789	DQ284111	AY948831	GQ345273	AY948932
Physalaemus/Engystomops		EF107462		EF107237	AY819096	EF107299
Leptodactylus	AY337266	AY364194	DQ284104	AY948838	DQ158259	AY364224
Calyptocephalella		EF107495	DQ284269	EF107275	AY819090	EF107334
Myobatrachidae	AY819262	EF107474	DQ284251	EF107251	AY819100	EF107310
Limnodynastidae	GQ345175	AY364189	DQ284415	AY523719	AY819099	AY364219
Ranidae		EF017988	DQ284312	EF018012	AY819103	DQ347231
Sequence Length (bp)	317	682	328	1282	531	556

continued.

Taxon	RAG-1 B	Rho	SIA	SLC8a3	Tyr
Melanophryniscus	AY844478	DQ283765	AY844899	AY948878	
Rhinella	AY844370	AY844547	AY844775	GQ345321	EF364358
Duttaphrynus	DQ158394	AF249097	DQ282815	AY948851	
Espadarana/Nymphargus	AY844371	AY844548	AY844776	AY948896	AY844029
Allophryne	AY844361	AY844538	AY844766		
Trachycephalus	AY844493	AY844707	AY844912	AY948880	AY844149
Hyla	AY844391	AY844577	AY844802	EF107393	AY844048
Acris	AY844358	AY844533	AY844762	EF107403	AY844019
Litoria	AY323767	AY844685	AY844893	AY948877	AY844131
Phyllomedusa	AY844496	AY844711	AY844916	AY948882	AY844153
Flectonotus	AY844379	AY844562	AY844788	GQ345322	AY844038
Stefania	AY844528	AY844756	AY844951	GQ345323	AY844353
Hemiphractus	AY844382	AY844566	AY844792	GQ345324	
Mannophryne/Allobates	DQ503345	DQ503236	DQ503097	GQ345325	DQ503136
Dendrobates/Hyloxalus	DQ503304	AY364395	AY844781	AY948879	DQ347160
Epipedobates	DQ503354	DQ283768	DQ503104	EF107381	DQ282902
Brachycephalus	GQ345290	DQ283808	DQ282673	GQ345326	DQ282919
Ischnocnema	GQ345291	DQ283809	GQ345308	GQ345327	EF493510
Craugastor	GQ345292	DQ283960	DQ282808	GQ345328	EF493481
Haddadus	GQ345293	DQ283807	GQ345309	GQ345329	DQ282918
Eleutherodactylus	GQ345294	DQ283937	GQ345310	EF107445	EF493455
Diasporus	GQ345295		GQ345311	GQ345330	EU186773
Adelophryne	GQ345296	GQ345302	GQ345312	GQ345331	EU186772
Pristimantis	DQ679272	AY844559	GQ345313	AY948898	EF493502
Phrynopus	GQ345297	GQ345303	GQ345314	GQ345332	EF493507
Hypodactylus	GQ345298	GQ345304	GQ345315	GQ345333	EF493484
Strabomantis	GQ345299		DQ282718	GQ345334	EU186775
Psychrophrynella	GQ345300		GQ345316	GQ345335	EU186776
Ceuthomantis-W1		GQ345305	GQ345317	GQ345336	
Ceuthomantis-W2			GQ345318	GQ345337	
Ceuthomantis-A		GQ345306	GQ345319	GQ345338	
Batrachyla	AY844369	AY844546	AY844774	AY948899	AY844028
Ceratophrys	DQ679269	AY364399		AY948886	DQ347168
Lepidobatrachus	DQ679270	DQ283851	DQ282707	EF107386	
Telmatobius	AY844529	AY844757	AY844952	EF107389	DQ347182
Odontophrynus/Proceratophrys	AY844480	AY844695	AY844901	AY948897	DQ282903
Thoropa	GQ345301	GQ345307	GQ345320	GQ345339	

Rhinoderma/Cycloramphus	DQ503357	DQ283963	DQ282813	AY948895	DQ282924
Hylodes	DQ503367	DQ503253	DQ503119	GQ345340	DQ282923
Pleurodema	AY844503	AY844721	AY844926	AY948888	
Physalaemus/Engystomops	AY844499	AY844717	DQ282875	EF107387	
Leptodactylus	AY844470	AY844681	AY844890	AY948900	DQ347193
Calyptocephalella	AY583337	DQ284036	DQ282893	EF107440	
Myobatrachidae		DQ283955	DQ282758	EF107410	DQ282965
Limnodynastidae	AY583341	DQ283954	DQ282805	AY948889	
Ranidae	AY323776	AF249119	DQ282735	EF107369	AF249182
Sequence Length (bp)	428	316	397	1111	532